Aus der Anatomischen Anstalt Lehrstuhl II – Neuroanatomie
der
Ludwig-Maximilians-Universität
München

Vorstand: Prof. Dr. Christoph Schmitz

NRF2 als Regulator der integrated stress response in Oligodendrozyten

Dissertation
zum Erwerb des Doktorgrades der Medizin
an der Medizinischen Fakultät der
Ludwig-Maximilians-Universität zu München

vorgelegt von

Nico Teske
aus Dortmund
2021

Mit Genehmigung der Medizinischen Fakultät
der Universität München

Berichterstatter:	Prof. Dr. Dr. Markus Kipp
Mitberichterstatter:	PD Dr. Rupert Egensperger Prof. Dr. Martin Kerschensteiner Prof. Dr. Hans-Walter Pfister
Dekan:	Prof. Dr. med. dent. Reinhard Hickel
Tag der mündlichen Prüfung:	10.06.2021

Kumulative Dissertation gemäß § 4a der Promotionsordnung

1. Eidesstattliche Versicherung

Name, Vorname: Teske, Nico

Ich erkläre hiermit an Eides statt,
dass ich die vorliegende Dissertation mit dem Thema

„NRF2 als Regulator der integrated stress response in Oligodendrozyten“

selbstständig verfasst, mich außer der angegebenen keiner weiteren Hilfsmittel bedient und alle Erkenntnisse, die aus dem Schrifttum ganz oder annähernd übernommen sind, als solche kenntlich gemacht und nach ihrer Herkunft unter Bezeichnung der Fundstelle einzeln nachgewiesen habe.
Ich erkläre des Weiteren, dass die hier vorgelegte Dissertation nicht in gleicher oder in ähnlicher Form bei einer anderen Stelle zur Erlangung eines akademischen Grades eingereicht wurde.

München, den 12.06.2021 Nico Teske

Inhaltsverzeichnis

2. Abkürzungsverzeichnis

ARE	antioxidant response element
ATF3	activating transcription factor 3
ATF4	activating transcription factor 4
ATF6	activating transcription factor 6
CNS	central nervous system
DDIT3	DNA damage−inducible transcript 3 protein
eIF2α	eukaryotic initiation factor 2 alpha
ER	Endoplasmatisches Retikulum
GDF15	growth/differentiation factor 15
Grp94	glucose-regulated protein 94
IL-6	Interleukin 6
IL-8	Interleukin 8
IRE1	inositol requiring 1
ISR	integrated stress response
KEAP1	Kelch ECH−associated protein 1
MS	Multiple Sklerose
NOS2	nitric oxide synthase-2
NRF2	nuclear factor (erythroid-derived 2)-like 2
OPC	Oligodendrozyten-Progenitorzelle
PERK	protein kinase RNA-like endoplasmic reticulum kinase
ROS	reactive oxygen species
UPR	unfolded protein response
XBP1	X-box binding protein 1
ZNS	Zentralnervensystem

3. Publikationsliste

1. Nico Teske, Annette Liessem, Felix Fischbach, Tim Clarner, Cordian Beyer, Christoph Wruck, Athanassios Fragoulis, Simone C. Tauber, Marion Victor and Markus Kipp, Chemical hypoxia-induced integrated stress response activation in oligodendrocytes is mediated by the transcription factor nuclear factor (erythroid-derived 2)-like 2 (NRF2)., Journal of Neurochemistry 144:285–301. doi: 10.1111/jnc.14270, (2018).

2. Miriam Scheld, Athanassios Fragoulis, Stella Nyamoya, Adib Zendedel, Bernd Denecke, Barbara Krauspe, Nico Teske, Markus Kipp, Cordian Beyer and Tim Clarner, Mitochondrial Impairment in Oligodendroglial Cells Induces Cytokine Expression and Signaling, Journal of Molecular Neuroscience, doi: 10.1007/s12031-018-1236-6, (2018).

4. Einleitung

Oligodendrozyten sind die myelinisierenden Zellen des Zentralnervensystems (ZNS). Sie unterliegen einer komplexen Zellproliferation, -migration und -differenzierung, die in der Ausbildung der Myelinscheide der Axone zentraler Neurone endet. Um die Versorgung und Erregungsleitung der Axone des ZNS sicherzustellen, sind Oligodendrozyten dazu in der Lage durch einen extrem gesteigerten Metabolismus jeden Tag große Mengen Myelin zu produzieren. Auf Grund der komplexen Differenzierung und einzigartigen Physiologie stellen sie eine vulnerable Zellpopulation im ZNS dar (Bradl & Lassmann 2010). Störungen dieser Zelllinie sind mit einer Vielzahl von Erkrankungen des ZNS assoziiert, unter anderem mit der Multiplen Sklerose (MS) (Barnett & Prineas 2004; Prineas & Parratt 2012; Kipp et al. 2017), dem Schlaganfall (Pantoni et al. 1996; di Penta et al. 2013), Rückenmarksverletzungen (Li et al. 1999), der Schizophrenie (Vostrikov et al. 2008) und bipolar-affektiven Störungen (Uranova et al. 2001). Oxidativer Stress stellt eine der vielen Ursachen für Oligodendrozytensterben dar (Haider et al. 2011; di Penta et al. 2013; Rosenzweig & Carmichael 2013; Liu et al. 2014). In humanen MS-Läsionen konnte post mortem gesteigerter Zelltod von reifen Oligodendrozyten nachgewiesen werden (Prineas & Parratt 2012). In Biopsien von humanen MS-Läsionen konnte gesteigerter Zelltod von Oligodendrozyten-Progenitorzellen (OPC)s nachgewiesen werden (Cui et al. 2013). Oligodendrozyten-Progenitorzellen sind maßgeblich am Prozess der Remyelinisierung beteiligt. OPC Aktivierung, Proliferation und Migration hin zu demyelinisierten Axonen stellen dabei notwendige Schritte dar. Vor Ort differenzieren die Progenitorzellen aus und remyelinisieren Axone, deren Myelinscheiden geschädigt wurden. In MS Patienten ist diese endogene Remyelinisierung meist unvollständig (Patrikios et al. 2006). Zudem nimmt die Effektivität im Alter ab (Sim et al. 2002). Die Remyelinisierung stellt eine effektive Möglichkeit der Gewebereparatur dar. Ihr werden neuroprotektive Effekte zugeschrieben (Bramow et al. 2010; Bruce et al. 2010), weshalb sie intensiv im Hinblick auf neue therapeutische Strategien erforscht wird (Plemel et al. 2017). Ein besseres Verständnis von OPC-Pathologien und beteiligter Signalwege ist unabdingbar mit diesen Strategien verbunden.

Ein Beispiel für eine solche Signalkaskade ist die unfolded protein response (UPR), eine Reihe adaptiver Signalwege, die zusammen bei einer Ansammlung un- oder fehlgefalteter Proteine innerhalb des endoplasmatischen Retikulums (ER) zur Expressions-Induktion spezifischer ER Chaperone führen (Kozutsumi et al. 1988). Diese Signalkaskade kontrolliert die ER-Homöostase, welche insbesondere in sekretorisch aktiven Zellen, wie Plasmozyten, Hepatozyten und

pankreatischen β-Zellen eine wichtige Rolle spielt. Die UPR kann durch drei verschiedene ER-Transmembranproteine aktiviert werden: inositol requiring 1 (IRE1), protein kinase RNA-like endoplasmic reticulum kinase (PERK) und activating transcription factor 6 (ATF6). IRE1 aktiviert den Transkriptionsfaktor X-box binding protein 1 (XBP1), ATF6 den Transkriptionsfaktor ATF6 (N). Beide Signalzweige führen zu einer selektiven Expressions-Induktion von zytoprotektiven Proteinen. PERK phosphoryliert eukaryotic initiation factor 2 alpha (eIF2 α). Dies führt zum einen zu einer selektiven Expressions-Induktion von zytoprotektiven Proteinen und Chaperonen wie zum Beispiel glucose-regulated protein 94 (Grp94) (Liu & Li 2008). Zum anderen führt die Phosphorylierung von eIF2 α zu einer gehemmten Translation und damit zu einer verminderten Proteinbiosynthese (Smith & Mallucci 2016). Bei persistierendem Zellstress führen DNA damage-inducible transcript 3 protein (DDIT3) (Rutkowski et al. 2006; Puthalakath et al. 2007) und activating transcription factor 3 (ATF3) (Edagawa et al. 2014) zur Apoptose.

Eine gestörte Proteinfaltung stellt jedoch nicht den einzigen Weg der Aktivierung einer unfolded protein response dar. Verschiedene zelluläre Veränderungen, wie zum Beispiel ein Mangel von Aminosäuren oder Glucose oder aber eine Hypoxie, können vor allem über PERK ebenfalls eine UPR Aktivierung induzieren, weshalb man hier von einer integrated stress response (ISR) spricht (Pakos-Zebrucka et al. 2016). Oxidativer Stress wird ebenfalls mit der ISR in Verbindung gebracht. So konnte gezeigt werden, dass die Redox-Homöostase eine wichtige Rolle in Faltungsprozessen von Proteinen spielt (van der Vlies et al. 2003; Cao & Kaufman 2014) und die Produktion reaktiver Sauerstoffspezies (reactive oxygen species; ROS) von Teilen der ISR ausgelöst werden könnte (Santos et al. 2009). Zudem zeigte sich, dass die Zellprotektion bedingt durch Ddit3 Deletion teilweise auf Änderungen der Redox-Homöostase im ER zurückzuführen ist (Marciniak et al. 2004). Wenngleich ER-Stress und oxidativer Stress häufig in zellulären Pathologien gemeinsam vorkommen, ist bisher unklar in welchem Ausmaß oxidativer Stress und die ISR in Oligodendrozyten in Verbindung stehen.
Oxidativer Stress spielt eine bedeutende Rolle in der Pathogenese vieler neurodegenerativer und neuroinflammatorischer Erkrankungen, zum Beispiel dem Morbus Parkinson, dem Morbus Alzheimer (Lin & Beal 2006) oder der MS (Witte et al. 2014; Ohl et al. 2016). Dabei wird oxidativer Stress als ein Ungleichgewicht zwischen oxidierenden und reduzierenden Reaktionen innerhalb einer Zelle definiert, bei dem die oxidierenden Reaktionen überwiegen und die Produktion von ROS begünstigt wird. Obwohl ROS in geringen Konzentrationen physiologische Funktionen als sekundäre Botenstoffe erfüllen können (Reth 2002), führen höhere

Konzentrationen, welche die antioxidative Kapazität der Zelle übersteigen, zum Zusammenbruch der zellulären Redox-Homöostase. Die Folgen sind Schäden an Zellstrukturen wie Lipiden, Proteinen und Nukleinsäuren, die zur Beeinträchtigung zellulärer Abläufe und letztendlich zum Zelltod führen können.

Um oxidativem Stress entgegenzuwirken und sich vor Pro-Oxidantien zu schützen, haben alle Zellen intrinsische Mechanismen entwickelt, die überschüssige ROS neutralisieren können. Diese als oxidative stress response zusammengefassten Mechanismen werden maßgeblich durch den Transkriptionsfaktor nuclear factor (erythroid-derived 2)-like 2 (NRF2) reguliert. Im Ruhezustand wird NRF2 durch Kelch ECH−associated protein 1 (KEAP1) im Zytosol gebunden, ubiquitiniert und folglich abgebaut. Oxidativer Stress induziert Konformationsänderungen in KEAP1, wodurch NRF2 freigesetzt wird und in den Zellkern translozieren kann. Dort bindet es die DNA am sogenannten „antioxidant response element (ARE)“ und führt zu einer Transkriptions-Induktion antioxidativer Enzyme und Phase II Detox-Enzyme (Draheim et al. 2016; Itoh et al. 2003; Wakabayashi et al. 2003).

Gestresste Oligodendrozyten können unter anderem in der normal erscheinenden weißen Substanz (normal-appearing white matter) von MS Patienten gefunden werden. Dort kommen sie in so genannten „präaktiven Läsionen“ ((p)reactive lesions) zusammen mit Mikrogliaknötchen, kleinen Anhäufungen der residenten Immunzellen des ZNS, vor (De Groot et al. 2001; Zeis et al. 2009). Man geht davon aus, dass zumindest einige solcher präaktiven Läsionen den späteren aktiv-demyelinisierenden MS-Läsionen, die eine Störung der Blut-Hirn-Schranke und Infiltration von Lymphozyten aufzeigen, vorausgehen (Wuerfel et al. 2004; van der Valk & Amor 2009). Ruhende Mikrogliazellen können durch eine Vielzahl pathologischer Veränderungen im ZNS, z.B. durch Lymphozyten-Infiltration oder Anwesenheit von Mikroorganismen, aktiviert werden (Gehrmann et al. 1995; Perry et al. 1993). In vivo Modelle zeigen, dass das Ausmaß der Demyelinisierung zentraler Axone positiv mit der Anzahl aktivierter Mikrogliazellen korreliert (Clarner et al. 2012). Da in präaktiven Läsionen die Demyelinisierung, Leukozyten-Infiltration und weitere histopathologische Merkmale der klassischen MS-Läsionen fehlen (Gay et al. 1997; Barnett & Prineas 2004; van der Valk & Amor 2009), könnten in solchen Läsionen die gestressten Oligodendrozyten eine Rolle in der Mikrogliazell-Aktivierung spielen. Oligodendrozyten können eine Vielzahl von Signalmolekülen, die einen Einfluss auf immunologische Prozesse haben, sezernieren (Cannella & Raine 2004; Balabanov et al. 2007; Okamura et al. 2007; Tzartos et al. 2008; Moyon et al. 2015). Beispiele hierfür sind die humane

Oligodendrozyten Zelllinie MO3.13, die die Cytokine Interleukin-6 (IL6) und Interleukin-8 (IL8) in Anwesenheit von Borrelia burgdorferi sezerniert (Ramesh et al. 2012), oder primäre Ratten Oligodendrozyten, die eine gesteigerte Expression der Chemokine CXCL10, CCL2, CCL3 und CCL5 als Antwort auf Interferon-γ Behandlung zeigen (Balabanov et al. 2007).

4.1 Fragestellung

Die übergeordnete Fragestellung, welche die einzelnen Originalarbeiten miteinander verbindet, beschäftigt sich mit der Auswirkung von Oligodendrozyten-Pathologien in neurodegenerativen und neuroinflammatorischen Erkrankungen, insbesondere im Hinblick auf die Pathophysiologie von MS. Dabei sind sowohl die molekularbiologischen Zusammenhänge von oxidativem Stress und ER-Stress in Oligodendrozyten und ihren Vorläuferzellen, als auch die Auswirkungen dieser gestressten Zellen auf benachbarte Mikrogliazellen im Rahmen der Entstehung von MS-Läsionen von besonderem Interesse.

Im Rahmen der ersten Originalarbeit „Chemical hypoxia-induced integrated stress response activation in oligodendrocytes is mediated by the transcription factor nuclear factor (erythroid-derived 2)-like 2 (NRF2)“ wurde untersucht, ob Komponenten der ISR durch experimentelle Inhibition der Atmungskette aktiviert werden können. In einem weiteren Schritt sollte herausgefunden werden, ob diese Aktivierung unter Kontrolle von NRF2 steht. Dafür wurden die immortalisierten Oligodendrozyten-Zelllinien OLN93 und OliNeu als Modellsysteme verwendet. Das mitochondriale Membranpotenzial und ROS-Level wurden durchflusszytometrisch gemessen und dienten als Kontrolle für eine suffiziente Inhibition der Atmungskette. ER-Stress wurde durch Expressions-Induktion von Atf3, Atf4 und Ddit3 gemessen. Mittels lentiviralem Gen-Silencing von Nrf2 und Keap1 wurde die Rolle von NRF2 in der integrated stress response untersucht. Es konnte gezeigt werden, dass Hauptelemente der ISR, hier Atf3, Atf4 und Ddit3, in OPCs sowohl durch experimentelle ISR-Induktion als auch durch Inhibition der mitochondrialen Atmungskette (chemische Hypoxie) aktiviert werden. Zudem konnte gezeigt werden, dass die Expression von ATF3 und DDIT3 in dem in vivo Remyelinisierungsmodell Cuprizone (Slowik et al. 2015; Draheim et al. 2016) induziert wird. Die Expression von Atf3, Atf4 und Ddit3 durch Inhibition der Atmungskette zeigte sich ohne eine Aktivierung von Chaperonen (z.B. Grp94). NRF2 Überaktivierung mittels Keap1-Knockdown in OliNeu Zellen führte zu einer gesteigerten ISR-Aktivierung, wohingegen ein Nrf2-Knockdown eine reduzierte ISR-Aktivierung zeigte. Diese Ergebnisse zeigen eine funktionelle Verbindung zwischen dem

NRF2/ARE und dem ISR-Signalweg in OPCs auf. Daraus kann man schließen, dass oxidativer Stress eine ISR in Oligodendrozyten aktiviert und so möglicherweise die Degeneration von Oligodendrozyten in MS und anderen neurologischen Erkrankungen steuert.

Im Rahmen der zweiten Originalarbeit „Mitochondrial impairment in oligodendroglial cells induces cytokine expression and signaling“ wurde untersucht, welche Signalmoleküle von Oligodendrozyten unter oxidativem Stress sezerniert werden. Im nächsten Schritt wurde überprüft, ob die Signalmoleküle zu einer Mikrogliazell-Aktivierung führen und so die Entstehung präaktiver MS-Läsionen begünstigen können. Dafür wurden die Oligodendrozyten-Zelllinie OLN93 und die Mikroglia-Zelllinie BV2 als Modellsysteme verwendet. Oxidativer Stress wurde durch die Inhibition der Atmungskette mittels Sodium azide induziert. Mikrogliazell-Aktivierung wurde durch die Expressions-Induktion von nitric oxide synthase-2 (NOS2), einem proinflammatorischen Marker, und Arginase 1, einem antiinflammatorischen Marker, gemessen. Weiterhin wurde das Remyelinisierungsmodell Cuprizone verwendet, um die Genexpression von Oligodendrozyten in vivo zu untersuchen. Es konnte gezeigt werden, dass Oligodendrozyten-Progenitorzellen, nach Inhibition der mitochondrialen Atmungskette, eine selektiv gesteigerte Expression einer Vielzahl immunmodulierender Signalmoleküle aufzeigen. Oxidativer Stress induzierte unter anderem die Expression von IL-6, growth/differentiation factor 15 (GDF15) und einer Reihe weiterer Chemokine in vitro. IL-6 und GDF15 Expressions-Induktion konnte zudem in Gewebeschnitten von Cuprizone-behandelten Mäusen in dem in vivo Remyelinisierungsmodell Cuprizone nachgewiesen werden. Fluoreszenz-in-situ-Hybridisierung zeigte, dass unter anderem Oligodendrozyten für die IL-6 Expressions-Induktion im in vivo Modell verantwortlich sind. Inkubation von Mikrogliazellen mit konditioniertem Medium von gestressten Oligodendrozyten führte zu einer gesteigerten Expression von NOS2 und Arginase 1. IL-6-Antikörper vermittelte Blockierung von IL-6 unterdrückte diese Aktivierung unvollständig, sodass von weiteren Signalmolekülen ausgegangen werden muss, die zu einer Mikrogliazell-Aktivierung durch OPCs beitragen. Daraus kann man schließen, dass Oligodendrozyten das Potenzial haben Mikrogliazellen mit Hilfe verschiedener Cytokine und Chemokine zu aktivieren und auf diese Weise in der Entstehung von präaktiven MS-Läsionen eine Rolle spielen könnten.

4.2 Eigenanteil an der Arbeit

Bei der ersten Publikation mit dem Titel: „Chemical hypoxia-induced integrated stress response activation in oligodendrocytes is mediated by the transcription factor nuclear factor (erythroid-

derived 2)-like 2 (NRF2)“ setzte sich der Beitrag des Doktoranden an der Arbeit aus der Planung der Studie, der Durchführung der Experimente, der Datenauswertung, der Interpretation der Ergebnisse sowie der Verfassung der Veröffentlichung zusammen. Neben der Etablierung der Oligodendrozyten Zellkultur in der Anatomischen Anstalt München (Lehrstuhl 2 – Neuroanatomie), wurden die Zellviabilitäts-Assays, die Messungen der reaktiven Sauerstoffspezies und des Mitochondrienmembranpotenzials eigenständig durch den Doktoranden durchgeführt und ausgewertet. Der Doktorand wurde von seinen korrespondierenden Autoren bei der Daten- und Statistikerhebung der Zelltransfektions-Experimente, Genexpressionsanalysen, Western Blots und in vivo Experimente, sowie der Überarbeitung des Manuskripts unterstützt. Zusätzlich hatte der Doktorand regelmäßigen Kontakt mit seinem betreuenden Doktorvater, der ihm bei speziellen Fragestellungen sowie der Korrektur des Manuskripts unterstützt hat. Aus diesem wesentlichen Anteil ergibt sich die Stellung als Erstautor dieser Publikation.

Bei der zweiten Publikation mit dem Titel: „Mitochondrial impairment in oligodendroglial cells induces cytokine expression and signaling“ setzte sich der Beitrag des Doktoranden an der Arbeit aus der Anwendung der bereits etablierten Methoden der Zellkultur, der Datenauswertung, der Interpretation der Ergebnisse sowie der Überarbeitung des Manuskripts zusammen. Dabei wurden die CellTiter-Blue® Zellviabilitäts-Assays und die CytoTox 96® Zelltoxizitäts-Assays selbstständig vom Doktoranden durchgeführt (Scheld et al. 2018, Fig. 1a). Daraus ergibt sich die Stellung der Ko-Autorenschaft in dieser Publikation.

5. Zusammenfassung

Die genauen pathophysiologischen Mechanismen vieler neurodegenerativer und neuroinflammatorischer Erkrankungen sind nach wie vor nicht hinreichend geklärt. Dazu zählen unter anderem die Entstehung von Läsionen im Rahmen der Multiplen Sklerose sowie die unvollständige Remyelinisierung entmarkter Läsionen in MS Patienten. Oligodendrozyten-Pathologien scheinen in beiden Szenarien eine entscheidende Rolle zu spielen. Insbesondere Beeinträchtigungen von Oligodendrozyten-Progenitorzellen sind im Prozess der unvollständigen Remyelinisierung involviert und können unter anderem durch oxidativen Stress ausgelöst werden.

Die beiden Publikationen dieser kumulativen Dissertation beschäftigen sich mit den molekularbiologischen Mechanismen von Oligodendrozyten und ihren Vorläuferzellen in diesem Zusammenhang. Die erste Publikation konnte zeigen, dass Hauptelemente einer integrated stress response, hier Atf3, Atf4 und Ddit3 in Oligodendrozyten-Progenitorzellen sowohl durch experimentelle ISR-Induktion als auch durch Inhibition der mitochondrialen Atmungskette (chemische Hypoxie) aktiviert werden. Konstitutive Überaktivierung des Transkriptionsfaktors NRF2 mittels Keap1-Knockdown in OliNeu Zellen führte zu einer gesteigerten ISR-Aktivierung, wohingegen ein Nrf2-Knockdown eine reduzierte ISR-Aktivierung zeigte. Im Rahmen der zweiten Publikation untersuchten wir die Expression von Signalmolekülen durch Oligodendrozyten, die zu einer Mikrogliazell-Aktivierung in präaktiven MS-Läsionen führen könnten. Oligodendrozyten-Progenitorzellen, deren mitochondriale Atmungskette experimentell inhibiert wurde, zeigten eine selektiv gesteigerte Expression von immunmodulierenden Signalmolekülen, unter anderem von Interleukin 6. Eine gesteigerte IL-6 Expression durch Oligodendrozyten konnte ebenfalls in einem in vivo Remyelinisierungsmodell nachgewiesen werden. In vitro führte die Inkubation von Mikrogliazellen mit konditioniertem Medium von gestressten Oligodendrozyten zu einer gesteigerten Expression von nitric oxide synthase-2 und Arginase 1, zwei Markern für eine Mikrogliazell-Aktivierung.

Zusammenfassend konnten wir in Rahmen der beiden vorgelegten Arbeiten zeigen, dass (1) oxidativer Stress eine ISR in Oligodendrozyten aktiviert, und dass (2) diese gestressten Oligodendrozyten das Potenzial haben Mikrogliazellen mit Hilfe verschiedener Signalmoleküle zu aktiveren und so möglicherweise die Degeneration von Oligodendrozyten und die Entstehung von präaktiven Läsionen bei der Multiple Sklerose gesteuert wird.

6. Summary

The precise pathophysiological mechanisms underlying neurodegenerative and neuroinflammatory disorders among multiple sclerosis (MS) are still poorly understood. In MS, the pathogenesis of lesion formation in patients and their incomplete remyelination, respectively, are of great interest. In both scenarios, oligodendrocyte pathologies appear to be involved. Injury to oligodendrocyte progenitor cells caused by cellular disturbances like oxidative stress can be a contributing factor for such incomplete remyelination.

Both publications describe the molecular biological mechanisms in oligodendrocyte pathologies in this context. The first publication showed that the induction of distinct elements of an integrated stress response, namely activating transcription factor 3 and 4 and DNA damage−inducible transcript 3 protein, is activated in oligodendrocyte progenitor cells as a result of experimental ISR induction as well as inhibition of the respiratory chain (chemical hypoxia). Hyperactivation of NRF2 by Keap1 knockdown led to an increased ISR activation. Nrf2 deficient cells, however, showed decreased ISR activation. The second publication describes the expression of signaling molecules by oligodendrocytes, which could potentially lead to a microglia activation in preactive MS lesions. Oligodendrocyte progenitor cells, stressed by inhibition of the respiratory chain, showed expression induction of distinct immune modulating molecules, such as interleukin 6. IL-6 expression induction by oligodendrocytes was also demonstrated in a in vivo remyelination model. In vitro, microglia incubation with oligodendrocyte conditioned medium led to expression induction of nitric oxide synthase-2 und arginase 1, both key markers for microglia activation. In conclusion, the publications could show that (1) oxidative stress activates an ISR in oligodendrocytes and (2) stressed oligodendrocytes are capable of activating microglia by means of a cytokine mixture, thus contributing in oligodendrocyte degeneration and preactive lesion formation in MS.

7. Veröffentlichung I

Nico Teske, Annette Liessem, Felix Fischbach, Tim Clarner, Cordian Beyer, Christoph Wruck, Athanassios Fragoulis, Simone C. Tauber, Marion Victor and Markus Kipp, Chemical hypoxia-induced integrated stress response activation in oligodendrocytes is mediated by the transcription factor nuclear factor (erythroid-derived 2)-like 2 (NRF2)., Journal of Neurochemistry 144:285–301. doi: 10.1111/jnc.14270, (2018).

Journal of Neurochemistry

JOURNAL OF NEUROCHEMISTRY | 2018 | 144 | 285–301 doi: 10.1111/jnc.14270

ORIGINAL ARTICLE

Chemical hypoxia-induced integrated stress response activation in oligodendrocytes is mediated by the transcription factor nuclear factor (erythroid-derived 2)-like 2 (NRF2)

Nico Teske,* Annette Liessem,† Felix Fischbach,* Tim Clarner,† Cordian Beyer,† Christoph Wruck,‡ Athanassios Fragoulis,‡ Simone C. Tauber,§ Marion Victor¶,[1] and Markus Kipp*,[1]

*Department of Anatomy II, Ludwig-Maximilians-University of Munich, Munich, Germany
†Institute of Neuroanatomy and JARA-BRAIN, Faculty of Medicine, RWTH Aachen University, Aachen, Germany
‡Department of Anatomy and Cell Biology, RWTH Aachen University, Aachen, Germany
§Department of Neurology, RWTH University Hospital Aachen, Aachen, Germany
¶Institute of Anatomy II, Medical Faculty, Heinrich-Heine-University, Düsseldorf, Germany

Abstract

The extent of remyelination in multiple sclerosis lesions is often incomplete. Injury to oligodendrocyte progenitor cells can be a contributing factor for such incomplete remyelination. The precise mechanisms underlying insufficient repair remain to be defined, but oxidative stress appears to be involved. Here, we used immortalized oligodendrocyte cell lines as model systems to investigate a causal relation of oxidative stress and endoplasmic reticulum stress signaling cascades. OLN93 and OliNeu cells were subjected to chemical hypoxia by blocking the respiratory chain at various levels. Mitochondrial membrane potential and oxidative stress levels were quantified by flow cytometry. Endoplasmic reticulum stress was monitored by the expression induction of activating transcription factor 3 and 4 (Atf3, Atf4), DNA damage-inducible transcript 3 protein (Ddit3), and glucose-regulated protein 94. Lentiviral silencing of nuclear factor (erythroid-derived 2)-like 2 or kelch-like ECH-associated protein 1 was applied to study the relevance of NRF2 for endoplasmic reticulum stress responses. We demonstrate that inhibition of the respiratory chain induces oxidative stress in cultured oligodendrocytes which is paralleled by the expression induction of distinct mediators of the endoplasmic reticulum stress response, namely Atf3, Atf4, and Ddit3. Atf3 and Ddit3 expression induction is potentiated in kelch-like ECH-associated protein 1-deficient cells and absent in cells lacking the oxidative stress-related transcription factor NRF2. This study provides strong evidence that oxidative stress in oligodendrocytes activates endoplasmic reticulum

Received November 3, 2017; revised manuscript received November 18, 2017; accepted November 20, 2017.

Address correspondence and reprint requests to Markus Kipp, Anatomische Anstalt; Lehrstuhl II – Neuroanatomie, Pettenkoferstr. 11; 80336 München, Germany.
E-mail: markus.kipp@med.uni-muenchen.de

[1]These authors contributed equally as last authors.

Abbreviations used: ADP, adenosine diphosphate; APC, adenomatous polyposis coli; ARE, antioxidant response element; Atf3, activating transcription factor 3; Atf4, activating transcription factor 4; Atf6, activating transcription factor 6; ATP, adenosine triphosphate; BSA, bovine serum albumin; CNS, central nervous system; Ddit3, DNA damage-inducible transcript 3 protein; DMEM, Dulbecco's modified Eagle's medium; DMSO, dimethyl sulfoxide; EAE, experimental autoimmune encephalomyelitis; eIF2a, eukaryotic initiation factor 2 alpha; ER, endoplasmic reticulum; FADH2, flavin adenine dinucleotide; FBS, fetal bovine serum; Grp94, glucose-regulated protein 94; IRE1, inositol requiring 1; ISR, integrated stress response; Keap1, kelch-like ECH-associated protein 1; LDH, lactate dehydrogenase; MS, multiple sclerosis; NADH, nicotinamide adenine dinucleotide; Nrf2, nuclear factor (erythroid-derived 2)-like 2; OLIG2, oligodendrocyte transcription factor 2; OPC, oligodendrocyte progenitor cell; PBS, phosphate-buffered saline; PDL, poly-D-lysin; PERK, protein kinase RNA-like endoplasmic reticulum kinase; PFA, paraformaldehyde solution; PLP, proteolipid protein; RRID, research resource identifiers (see https://scicrunch.org/); ROS, reactive oxygen species; RT rt-PCR, reverse transcription real time-PCR technology; SDS, sodium dodecyl sulfate; TBS, Tris-buffered saline; TBST, TBS-Tween; UPR, unfolded protein response.

ORIGINAL ARTICLE

stress response in a NRF2-dependent manner and, in consequence, might regulate oligodendrocyte degeneration in multiple sclerosis and other neurological disorders.

Keywords: chemical hypoxia, ISR, multiple sclerosis, Nrf2, oligodendrocytes.
J. Neurochem. (2018) 144, 285--301.

Oligodendrocytes are the myelinating cells of the central nervous system (CNS). They have to undergo a complex program of proliferation, migration, differentiation, and myelination to finally produce the axonal myelin sheaths. Because of this complex differentiation program and their unique metabolism/physiology, oligodendrocytes represent a vulnerable cell population within the CNS. Disturbance of oligodendrocyte development and maintenance is associated with major diseases of the CNS including multiple sclerosis (MS) (Barnett and Prineas 2004; Prineas and Parratt 2012; Kipp et al. 2017), stroke (Pantoni et al. 1996; Fern et al. 2014), spinal cord injury (Li et al. 1999), schizophrenia (Vostrikov et al. 2008), and bipolar psychiatric disorders (Uranova et al. 2001). Underlying mechanisms causing oligodendrocyte damage are manifold including hypoxia (Scheuer et al. 2015), inflammation (di Penta et al. 2013; Rosenzweig and Carmichael 2013), glutamate excitotoxicity (Pitt et al. 2000; Matute et al. 2007), and oxidative stress (Haider et al. 2011; di Penta et al. 2013; Rosenzweig and Carmichael 2013; Liu et al. 2014). Of note, in MS which is the best studied disease related to oligodendrocyte pathology, mature oligodendrocytes (Prineas and Parratt 2012) as well as oligodendrocyte progenitor cells (Cui et al. 2013) show increased cell death. Preservation of both cell entities is still an unmet medical need.

Remyelination is one of the best documented and most robust examples of tissue repair in the CNS. Although in the adult brain, the regeneration of destroyed neurons is very limited, lost myelin sheaths can principally very effectively be repaired. On the cellular levels, steps involved in remyelination include the activation and proliferation of oligodendrocyte progenitor cells (OPCs), the migration of these OPCs toward the demyelinated axon, and the interaction of OPCs with the axon, which culminates in OPC differentiation and finally remyelination. The beneficial effects of remyelination are well known and include the restoration of axonal conduction properties that are lost following demyelination (Honmou et al. 1996) as well as axonal protection (Funfschilling et al. 2012; Moore et al. 2013; Schampel et al. 2017). For reasons that are not well understood, remyelination is incomplete in most of MS patients (Patrikios et al. 2006), and remyelination efficacy decreases with age (Sim et al. 2002). Because of the believed neuroprotective effect of remyelination (Patrikios et al. 2006; Bramow et al. 2010; Bruce et al. 2010), new therapeutic strategies aimed at promoting remyelination are currently intensively tested. Although it has been shown that the impairment of both, OPC recruitment and differentiation, might be attributable to the failure of remyelination in MS patients and its animal models (Chang et al. 2000, 2002; Sim et al. 2002), OPC death during the remyelination process has been suggested to contribute to remyelination failure (Natarajan et al. 2013; Simonishvili et al. 2013; Maus et al. 2015; Moore et al. 2015; Dincman et al. 2016). Since successful remyelination within the injured CNS is largely dependent on the survival of OPCs, a better understanding of pathways involved during OPC injury is urgently needed.

A groundbreaking study that was published more than two decades ago highlighted the existence of an adaptive pathway in mammalian cells that controls response to protein folding stress through the transcriptional activation of genes coding for essential endoplasmic reticulum (ER) chaperones (Kozutsumi et al. 1988). This adaptive response was termed unfolded protein response (UPR). In consequence, the UPR has been associated with the maintenance of cellular homeostasis in specialized secretory cells, including plasmocytes, hepatocytes, and pancreatic b-cells in which the secretory protein folding burden constitutes a constant source of stress. Classically, UPR is initiated by three ER transmembrane proteins: inositol requiring 1, protein kinase RNA-like endoplasmic reticulum kinase (PERK), and activating transcription factor 6. The focal point of UPR induction is the phosphorylation of eukaryotic initiation factor 2 alpha (eIF2a), diminishing global translation while selectively up-regulating the translation of chaperones such as glucose-regulated protein 94 (Grp94) (Liu and Li 2008) and other cytoprotective proteins. If cell stress persists, DDIT3 (Rutkowski et al. 2006; Puthalakath et al. 2007) and other components of the UPR such as ATF3 (Edagawa et al. 2014) can mediate apoptosis.

Cellular responses controlled by the UPR signaling branches are not solely restricted to protein folding stress. Especially activation of the PERK signaling pathway can occur in response to a range of physiological changes and pathological conditions, including amino acid deprivation, glucose deprivation, or hypoxia (Pakos-Zebrucka et al. 2016), and was therefore termed integrated stress response (ISR). The common point of convergence for all the stress stimuli that activate the ISR is the phosphorylation of eIF2a on serine 51.

Several studies support the view that, for example, oxidative stress has a strong connection with the ISR. In support of this assumption, it has been demonstrated that redox homeostasis is crucial for the protein folding process and disulfide bond formation within the ER (van der Vlies

et al. 2003). Furthermore, exogenous oxidants such as reactive oxygen species (ROS) produced by peroxides, metal ions, and lipid oxidation products may activate ISR branches (reviewed in (Cao and Kaufman 2014; Santos et al. 2009)). Finally, it has been shown that Ddit3 deletion protects cells partially by changing redox conditions within the ER (Marciniak et al. 2004). To what extent such an oxidative-ISR crosstalk exists in oligodendrocytes is not well understood.

Oxidative stress plays a major role in the pathogenesis of neurodegenerative and neuroinflammatory disorders among MS (Witte et al. 2014; Ohl et al. 2016). Oxidative stress arises when the production of ROS overwhelms the intrinsic antioxidant defense machinery. Principally, ROS play important roles as second messengers in many intracellular signaling cascades aimed at maintaining cellular homeostasis. At higher levels, ROS can cause indiscriminate damage to biological molecules leading to loss of function and even cell death. Thus, oxidative stress reflects an imbalance between the systemic manifestation of ROS and the ability of a biological system to readily detoxify the reactive intermediates or to repair the resulting damage (Ohl et al. 2016). All cells are equipped with an intrinsic mechanism that neutralizes excess ROS and protects against oxidative injury. This so-called oxidative stress response is mainly, but not exclusively, controlled by the transcription factor nuclear factor (erythroid-derived 2)-like 2 (NRF2). Under quiescent conditions, NRF2 is retained and degraded in the cytosol by Kelch ECH-associated protein 1 (KEAP1). If oxidative stress is present within a cell, NRF2 is released from KEAP1 and translocates into the nucleus where it binds to the antioxidant response element (ARE), thereby activating the transcription of antioxidant and detoxifying enzymes (Itoh et al. 2003; Wakabayashi et al. 2003; Draheim et al. 2016).

In this work, we show that key elements of an ISR, namely Atf3, Atf4, and Ddit3, are induced in OPCs through experimental ISR induction and, equally, by inhibition of respiratory chain activity (i.e., chemical hypoxia), which is paralleled by ROS accumulation. Furthermore, ATF3 and DDIT3 are expressed in OPCs in the in vivo remyelination model cuprizone. Induction of Atf3, Atf4, and Ddit3 expression by mitochondrial chain inhibitors occurred despite the absence of chaperone induction (i.e., Grp94). Hyperactivation of NRF2-signaling by Keap1 knockdown boosted ISR induction, whereas blocking of the oxidative stress response by Nrf2 knockdown prevented ISR induction in cultured oligodendrocytes. These results illustrate a functional crosstalk between the NRF2/ARE and ISR pathways in OPCs.

Material and methods

OLN93 cell culture and treatment

We received cells of the oligodendroglial cell line OLN93 from Dr C. Richter-Landsberg (RRID:CVCL_5850; Oldenburg, Germany) (Richter-Landsberg and Heinrich 1996). Cell lines were not authenticated prior to experiments. None of the cell lines used in these experiments are listed as a commonly misidentified cell line by the International Cell Line Authentication Committee. For propagation, cells were grown in 75 cm^2 plastic cell culture flasks in Dulbecco's modified Eagle's medium with 4.5 g/L D-Glucose, sodium pyruvate and L-glutamine (DMEM, Gibco, Rockville, MD, USA, order numb. 41966-029), and were supplemented with 1% penicillin/streptomycin (Gibco Life Technologies, order numb. 15140-122), and 10% fetal bovine serum (FBS, Gibco Life Technologies, order numb. 10500-064). Cells were cultured at 37°C in a humidified, 5% CO_2 atmosphere with medium replenishment every 2–3 days during cell maintenance. For experiments, cells were seeded onto 1.9 (~5 9 10^4 cells) or 9.6 cm^2 (~5x10^5 cells) plastic culture dishes pre-coated with 10 lg/mL poly-D-lysin (MW 70 000–150 000, Sigma, St Louis, MO, USA, order numb. P6407) in modified SATO medium. Modified SATO is composed of DMEM with 1% N2 supplement (Gibco Life Technologies, order numb. 17502-048), 0.1% Tri-Iodo-thyronine (Sigma-Aldrich, Taufkirchen, Germany, order numb. T6397), 0.016% L-thyroxin (Sigma-Aldrich, order numb. T1775), and 0.05% gentamicin (Gibco Life Technologies, order numb. 15710049). For more details, see Table 1.

To analyze whether blocking of mitochondrial respiratory chain activity induces ISR activation, the following toxins were applied: rotenone (complex-I inhibitor; diluted in dimethyl sulfoxide; obtained from Sigma-Aldrich, order numb. R8875), antimycin (complex-III inhibitor; diluted in ethanol; obtained from Sigma-Aldrich, order numb. A8674), sodium azide (complex-IV inhibitor; diluted in H_2O; obtained from Sigma-Aldrich, order numb. S2002), and oligomycin (ATPase inhibitor; diluted in ethanol; obtained from Sigma-Aldrich, order numb. 75351). Mitochondrial chain inhibitors were dissolved according to the manufacturer's instructions in ultrapure water (obtained from Invitrogen, Carlsbad, CA, USA, order numb. 10977-035), ethanol (obtained from Sigma-Aldrich, order numb. 34923), or dimethyl sulfoxide (obtained from Sigma-Aldrich, order numb. D2438). Tunicamycin (diluted in ethanol; obtained from Sigma-Aldrich, order numb. T7765) which inhibits protein N-glycosylation was used to stimulate ISR activation. All toxins were prepared as stock solutions and properly stored, except sodium azide, which was always prepared freshly. Concentrations used for experiments are shown in the respective figure legends. No randomization was performed during cell treatment.

Primary oligodendrocyte cell culture

Primary rat oligodendrocyte cultures were established as published previously (Clarner et al. 2011). To verify that ISR induction is not an artifact in oligodendrocyte cell lines, primary rat oligodendrocyte cultures were treated with sodium azide (10 mM) or tunicamycin (25 lg/mL) for 24 h, and Atf3 and Ddit3 mRNA expression levels were determined by RT rt-PCR.

Cell viability assays

Lactate dehydrogenase (LDH) release was determined using the CytoTox 96 non-radioactive cytotoxicity assay (Promega, Germany, order numb. G1780) according to the manufacturer's instructions. Three wells per experiment were treated for 1 h with a lysis solution

Table 1 Composition of modified SATO medium

Supplements	Components	Preparation	Stock concentration	Volume for 100 mL medium	Final concentration
DMEM				98.8 mL	
N2 Supplement (1009)				1 mL	1%
	Human transferrin (Holo)		10 000 mg/L		100 mg/L
	Insulin recombinant full chain		500 mg/L		5 mg/L
	Progesterone		0.63 mg/L		6.3 lg/L
	Putrescine		1611 mg/L		16.11 mg/L
	Selenite		0.52 mg/L		5.2 lg/L
Tri-Iodo-Thyronine (TIT)		100 mg TIT dissolved in 297 mL EtOH	0.5 mM	100 lL	0.5 lM
L-Thyroxine		100 mg L-Thyroxine dissolved in 40 mL 0.13 M NaOH 70% EtOH	3.2 mM	16 lL	512 nM
Gentamicin			10 mg/mL	50 lL	5 lg/mL

Table 2 Primer sequences with appropriate annealing temperature and product size for the analysis of rat or mouse samples

Gene	Protein	Forward primer sequence Reverse primer sequence	AT [°C]	Product [bp]
Ddit3	CHOP	5′-CGGAACCTGAGGAGAGAGTG-3′ 5′-ATAGGTGCCCCCAATTTCAT-3′	59	200
Atf3	ATF3	5′-GACTGGTATTTGAAGCCAGTG-3′ 5′-GGACCGCATCTCAAAATAGC-3′	60	109
Atf4	ATF4	5′-GTTGGTCAGTGCCTCAGACA-3′ 5′-CATTCGAAACAGAGCATCGA-3′	57	109
Hspb90a1 (= Grp94)	GRP94	5′-TCTGGAACCAGCGAGTTTCT-3′ 5′-TTGGGTCAGCAATCACAGAG-3′	63	205
Keap1	Keap1	5′-GGCAGGACCAGTTGAACAGT-3′ 5′-CATAGCCTCCGAGGACGTAG-3′	60.5	138
Nrf2	Nrf2	5′-CCCAGCAGGACATGGATTTGA-3′ 5′-AGCTCATAGTCCTTCTGTCGC-3′	60.5	106

AT, annealing temperature; bp, base pairs

containing Triton X-100 to obtain maximum LDH release. Results are given as percentage LDH release related to maximum LDH release (i.e., Triton X-100 application). Metabolic activity was determined using the CellTiter-Blue cell viability assay (Promega, order numb. G8080). Treatment with lysis solution served as negative control. The average of fluorescence intensity of Triton X-100-treated cells was subtracted from fluorescence values obtained from cultured cells. Interference of Triton X-100 with fluorescence signals was excluded. Data are given in % of control absorbance values. No blinding was performed for the evaluation of these data. Experiments were performed with at least five biological and three technical replicates.

Gene expression analyses

For gene expression analyses, cells were treated for 24 h in modified SATO medium (see Table 1). Gene expression levels were measured using the reverse transcription real time-PCR technology (RT rt-PCR; Bio-Rad, Munich, Germany), SensiMix Plus SYBR plus Fluorescein (Quantace, Bioline, Luckenwalde, Germany, order numb. QT615-05), and a standardized protocol as described previously by our group. Experiments were performed with at least four biological and three technical replicates. Primer sequences and individual annealing temperatures are shown in Table 2. Relative quantification was performed using the DDCt method which results in ratios between target genes and the housekeeping reference gene cyclophilin A. Stable expression of this housekeeping gene under the shown experimental conditions was verified in pilot experiments. Melting curves and gel-electrophoresis of the PCR products were routinely performed to determine the specificity of the PCR reaction (data not shown). No blinding was performed for the evaluation of these data. For kinetic studies in OLN93 cells, cultures were treated for up to 24 h with sodium azide. Since no difference was observed for Atf3

and Ddit3 mRNA expression levels for early (2 h) and late (24 h) control cultures, values we pooled and statistically compared versus treatment groups.

Western blotting analyses

After treatment with thapsigargin (1 h; 300 nM), tunicamycin (2 h; 50 lg/mL), or sodium azide (2 h; 100 mM), OLN93 cells were rinsed with sterile phosphate-buffered saline (PBS) and lysed with ice-cold RIPA buffer (New England BioLabs, USA, order numb. 9806S) containing protease-inhibitor (New England BioLabs, order numb. 5871S) and phosphatase-inhibitor (New England BioLabs, order numb. 5870S). The protein concentration of each sample was semi-quantified using bovine serum albumin (BSA) as an internal standard (Thermo Fisher Scientific, München, Germany, order numb. 23209). Twenty microgram of protein were denatured in Laemmli buffer containing sodium dodecyl sulfate (pH = 6.8) and NuPage sample reducing agent (Thermo Fisher Scientific, order numb. NP0004). Proteins were separated in a 8–14% SDS-Page and transferred to nitrocellulose membranes. Blots were blocked in 5% BSA (Cell Signaling Technology, Beverly, MA, USA, order numb. 9998) in Tris-buffered saline (TBS) and after a rinsing step, incubated overnight (4°C) in primary antibodies directed against PERK (1 : 1000; Cell signaling, order numb. 3192, RRID: AB_2095847), phospho-PERK (1 : 1000; Cell signaling, order numb. 3179, RRID:AB_2095853), ATF4 (1 1000; Cell signaling, order numb. 11815, RRID:AB_2616025), eIF2a (1 : 1000; Cell signaling, order numb. 9722, RRID:AB_2230924), phospho-eIF2a (1 : 1000; Cell signaling, order numb. 9721, RRID:AB_330951), b-Tubulin (1 : 1000; Cell signaling, order numb. 2146, RRID: AB_2210545), or NRF2 (1 : 1000; Gentex, Irvine, CA, USA, order numb. GTX103322, RRID:AB_1950993) diluted in 5% BSA in TBS-Tween (TBST). Membranes were washed three times in TBST, followed by incubation in horseradish peroxidase-conjugated secondary anti-rabbit antibodies (1 : 1000; Cell signaling, order numb. 7074, RRID:AB_2099233), diluted in 5% BSA in TBST for 2 h at 19!C. After rinsing in TBST (three times), the signal was detected via chemiluminescence (SignalFire™ ECL Reagent; Cell signaling, order numb. 6883), and visualized with the FluorchemE (ProteinSimple; San Jose, CA, USA). Because of the shortened treatment interval, higher toxin concentrations were used (see respective figures).

Measurement of oxidative stress and mitochondrial membrane potential levels

Oxidative stress levels were quantified using the Muse™ Oxidative Stress Kit (Merck, Germany, order numb. MCH100111) together with the benchtop flow cytometry device Muse Cell Analyzer (Merck, Germany). Mitochondrial membrane potential was quantified using the Muse™ MitoPotential Kit (Merck, Germany, order numb. MCH100110). To this end, cells were seeded onto 1.9 (~5 9 10^4 cells; oxidative stress levels) or 9.6 cm^2 (~5 9 10^5 cells; membrane potential levels) plastic culture dishes pre-coated with 10 lg/mL poly-D-lysin in modified SATO medium. After 47 h, cells were exposed to the different respiratory chain inhibitors or tunicamycin for another 60 min and then harvested using TrypLE™ (Thermo Fisher Scientific, München, Germany) Express enzyme solution (Gibco Life Technologies, order numb. 12604039). Thereafter, cells were stained and flow cytometry analyses were performed according to the manufacturer's instruction. To avoid any bias, gating of the different cell populations was performed in a blinded manner. Experiments were performed with three biological and one technical replicate. Because of the shortened treatment interval, higher toxin concentrations were used (see respective figures).

In vivo experiments

Cuprizone-induced demyelination was performed as published previously by our group (Slowik et al. 2015; Draheim et al. 2016). In brief, 0.25 g cuprizone was weighed using precision scales and mechanically mixed with 100 g ground standard rodent chow using a commercial available kitchen machine (Kult X, WMF Group, Geislingen an der Steige, Germany). The chow was mixed at low speed and manual agitation for 1 min and was provided within the cage in two separate plastic Petri dishes. Experiments have been approved by Regierung Oberbayern (reference numbers 55.2-154-2532-73-15). A total of ten 7–8-week-old male C57Bl6J mice (Janvier, France; order numb. SC-CJ-8S-M; RRID: not registered) were used. Animals were allocated to groups applying the following procedure. First, animals were distributed across cages (five animals per cage; cage area 435 cm^2), in a manner that each group consisted of mice with comparable weight. Then, we picked cards numbered either 1 or 2 for the respective experimental group (1 = control, 2 = 5 weeks cuprizone). The number on the picked card randomly assigned the cages to the respective group.

Animals were kept under standard laboratory conditions (12 h light/dark cycle, controlled temperature 23 ! 2°C and 55% ! 10% humidity) with access to food and water ad libitum. It was ensured that researchers and technicians did not use any light during the night cycle period. Nestlets were used for environmental enrichment.

The following exclusion criteria were applied: severe weight loss (> 10% within 24 h), severe behavioral deficits (decreased locomotion, convulsions, stupor), or infections. No single animal met the exclusion criteria during the study.

For histological and immunohistochemical studies, mice were deeply anesthetized with ketamine (100 mg/kg i.p.) and xylazine (10 mg/kg i.p.) and transcardially perfused with ice-cold PBS followed by a 3.7% paraformaldehyde solution (pH 7.4). We did choose ketamine and xylazine because this combination provides an appropriate depth of anesthesia and analgesia without affecting important study parameters. No additional medication was given during experiments. We kept the number of animals used to a minimum. To this end, the in vivo material used during this study is currently used for other studies, and will be available for other research groups upon request to the authors. Brains were post-fixed overnight in paraformaldehyde, dissected, embedded in paraffin, and then coronal sections (5 lm) were cut. For immunohistochemistry, sections were rehydrated and, if necessary, antigens were unmasked with Tris/EDTA buffer (pH 9.0) or citrate (pH 6.0) heating. After washing in PBS, sections were incubated overnight (4°C) with anti-proteolipid protein antibodies to detect myelin [(PLP) 1 : 1000; Bio-Rad Laboratories, Hercules, CA, USA/AbD Serotec order numb. MCA839G, RRID:AB_2237198], with anti-adenomatous polyposis coli antibodies to detect mature oligodendrocytes ([APC; CC1] 1 : 200; Milipore, Burlington, Massachusetts, USA, order numb. OP80, RRID:AB_2057371), or with anti-oligodendrocyte transcription factor 2 antibodies to detect OPCs and mature oligodendrocytes ([OLIG2] 1 : 2000; Milipore, order numb. AB9610, RRID: AB_570666). The next day, slides were incubated with biotinylated

secondary antibodies for 1 h and then with peroxidase-coupled avidin-biotin complex (ABC kit; Vector Laboratories, Peterborough, UK) and treated with 3,3′-diaminobenzidine (DAKO, Hamburg, Germany) as a peroxidase substrate.

Immunoflourescence double labeling experiments were performed with the following combination of primary antibodies: (i) anti-OLIG2 (1 : 1000; Milipore, order numb. AB9610, RRID: AB_570666) combined with anti-DDIT3 (1 : 50; Abcam, Cambridge, UK, order numb. ab11419, RRID:AB_298023), or (ii) anti-OLIG2 (1 : 100; Millipore, order numb. MABN50, RRID: AB_10807410) combined with anti-ATF3 (1 : 200; Santa Cruz Biotechnology, Santa Cruz, CA, USA, order numb. sc-188, RRID: AB_2258513). Appropriate Alexa Fluor-coupled secondary antibodies (Life Technologies, Germany) were used to visualize the antigen-antibody complexes. To visualize DDIT3, we combined the anti-mouse biotinylated secondary antibody (1 : 200; Vector, order numb. BA-9200, RRID:AB_2336171) with Alexa Fluor 488-coupled Streptavidin (1 : 100; Invitrogen, order numb. S11223).

Cell transfection experiments

The murine oligodendroglial cell line OliNeu (RRID:CVCL IZ82) was cultured in SATO medium containing 2% FBS. SATO is composed of DMEM with 1% bovine serum albumin (BSA, Carl ROTH, order numb. CP84.2), 1% N2 supplement (Gibco Life Technologies, order numb. 17502-048), 1% penicillin/streptomycin (Gibco Life Technologies, order numb. 15140-122), 0.1% N-acetylcystein (Sigma-Aldrich, order numb. A9165), and 0.002% biotin (Sigma-Aldrich, order numb. B4639). Cell lines were not authenticated prior to experiments.

Nrf2 and Keap1 gene expression were silenced by lentiviral shRNA delivery. For that purpose, we used commercially available pLKO.1 vectors encoding shRNA sequences for either Nrf2 (TRC clone ID: TRCN0000054659) or Keap1 (TRC clone ID: TRCN0000099447). These vectors are part of the MISSION® (Sigma-Aldrich, Taufkirchen, Germany) shRNA contingent distributed by Sigma-Aldrich (Munich, Germany). For virus production, HEK 293T cells (ATCC® CRL-11268™) were co-transfected with the shRNA expression vector pLKO.1, the VSV-G envelope expressing pMD2.G construct (addgene, order numb. 12259) and the second generation lentiviral packaging plasmid psPAX2 (addgene, order numb. 12260). Transfection was conducted using jetPEI® (Polypus Transfection™, order numb. 101) transfection reagent according to the manufacturer's instruction. For transduction, cells were plated on poly-D-lysin-coated culture dishes in SATO supplemented with 2% FBS. The cells were exposed to the virus containing supernatant for 24 h. After 72 h, puromycin (Carl ROTH, order numb. 0240.1) was constantly supplemented to the medium at a concentration of 2 lg/mL to assure a sufficient selection of transduced cells. Control cells were transduced with a pLKO.1 construct expressing a shRNA without any target in mammals (pLKO.1-shNonTarget) to avoid data misinterpretation based on transduction side effects. Transfection efficacy was tested by analyzing Nrf2 and Keap1 mRNA expression levels by RT rt-PCR, as described above. Primer sequences and individual annealing temperatures are shown in Table 2. Beyond, NRF2 protein levels were determined by western blotting analyses as described above.

Statistical analyses

Statistical analyses were performed using Prism 5 (GraphPad Software Inc., San Diego, CA, USA). If not stated otherwise, at least two independent experiments were performed. All data are given as arithmetic means ± SEMs. A p value of $p \leq 0.05$ was considered to be statistically significant. Applied statistical tests are given in the respective figure legends. No outliers were excluded from the analyses. No sample size calculation was performed.

Results

Inhibition of the respiratory chain in cultured oligodendrocytes induces cell death

In a first set of experiments, we have exposed the oligodendrocyte cell line OLN93 to different concentrations of respiratory chain inhibitors to receive information about their cell toxicity, and to select toxin concentrations which do not result in cell death during the exposure period, but might be high enough to cause chemical hypoxia-induced oligodendrocyte stress. Viability of OLN93 cells was determined by analysis of LDH release into the cell culture supernatant and by measuring the metabolic activity in the same wells. As shown in Fig. 1, the application of all four inhibitors increased LDH release and decreased metabolic activity in higher concentrations, both indicating significant cell death. Concentrations exceeding 1 lM rotenone (Fig. 1a), 10 lM antimycin (Fig. 1b), 1 mM sodium azide (Fig. 1c), or 10 lM oligomycin (Fig. 1d) significantly reduced OLN93 metabolic activity, indicating an impaired cell metabolism at these concentrations.

Inhibition of the respiratory chain in cultured oligodendrocytes induces expression of ISR mediators

Next, we wanted to know whether inhibition of the respiratory chain in oligodendrocytes induces the activation of an ISR. To test for this, the respiratory chain was blocked at various levels, and the mRNA expression of four distinct ISR-related factors (i.e., Atf4, Atf3, Ddit3, and Grp94) was analyzed by RT rt-PCR. Based on our cell viability studies, the following toxin concentrations were applied: rotenone (1 lM), antimycin (10 lM), sodium azide (10 mM), and oligomycin (10 lM) (see arrows in Fig. 1). Furthermore, cells were treated with tunicamycin (50 lg/mL), which inhibits the formation of N-glycosidic linkages in glycoprotein synthesis and thus induces an ISR (Gillet et al. 2002). Since no significant difference of gene expression levels could be detected between control or vehicle-treated cultures (i.e., ethanol or dimethyl sulfoxide), values we pooled and statistically compared versus treatment groups. As shown in Fig. 2a, Atf4 mRNA expression was induced by all four respiratory chain inhibitors (rotenone +295 ± 29%; antimycin +563 ± 51%; sodium azide +381 ± 11%; oligomycin +491 ± 15%). The magnitudes of Atf4 mRNA expression induction were comparable to the effects of

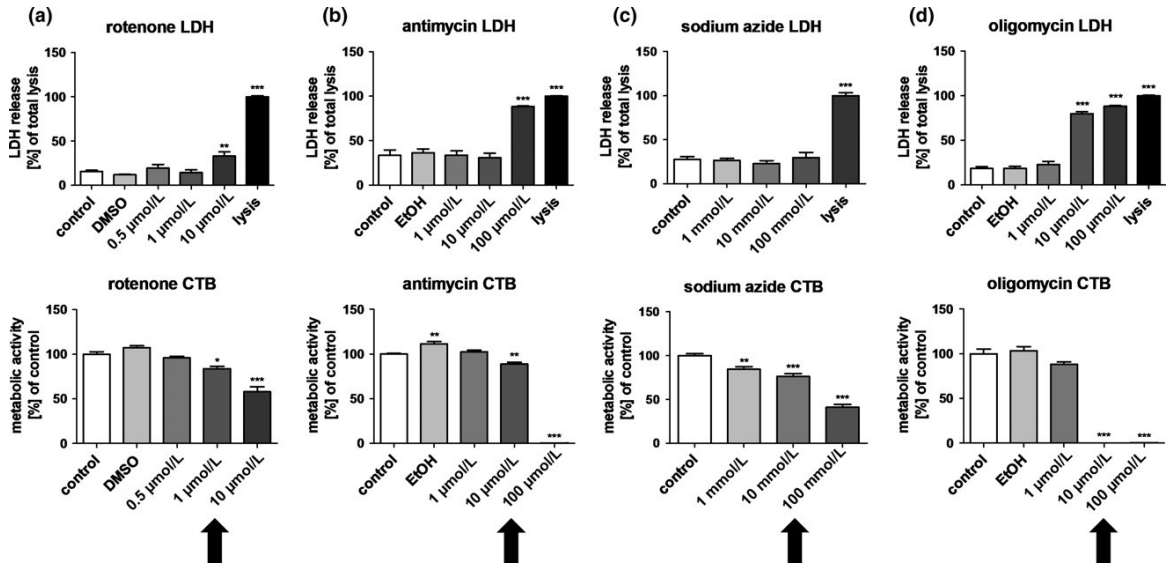

Fig. 1 Chemical hypoxia induces oligodendrocyte cell death. Effect of toxin administration (24 h) on metabolic activity and lactate dehydrogenase (LDH) release into the supernatant of cultured OLN93 cells. One representative experiment is shown (four culture wells; one representative experiment). Arrows highlight the toxin concentrations which were used in the following gene expression experiments. Comparison of cell viability measurements between control and treated cultures was done using one-way ANOVA with the obtained p-values corrected for multiple testing using the Dunnett's post hoc test. Significant differences with respect to control cultures are indicated by *$p < 0.05$, **$p < 0.01$, or ***$p < 0.001$.

tunicamycin (+774 ! 13%). Atf3 mRNA expression was significantly induced by rotenone (+622 ! 45%), antimycin (+1852 ! 331%), sodium azide (+463 ! 15%), and oligomycin (+29823 ! 4636%). Atf3 mRNA expression induction was as well pronounced in tunicamycin-treated cultures (+7741 ! 387%), but less intense compared to oligomycin ($p < 0.01$ oligomycin vs. tunicamycin). Ddit3 mRNA expression was significantly induced by antimycin (+2774 ! 323%), sodium azide (+1566 ! 104%), and oligomycin (+1950 ! 203%). Ddit3 mRNA expression was as well induced in rotenone (+918 ! 58%)-treated cultures, however, this differences was statistically not significant. The most pronounced effect on Ddit3 mRNA expression was observed for tunicamycin (+21894 ! 1026%). In contrast to Atf3, Atf4, and Ddit3, inhibition of the respiratory chain did not regulate the expression of the heat-shock protein Grp94. As expected, tunicamycin robustly induced Grp94 mRNA expression in cultured oligodendrocytes (+2006 ! 115%).

To test, whether ISR induction is a fast event, OLN93 cells were treated for up to 24 h with sodium azide, RNA isolated, and Ddit3 and Atf3 mRNA expression levels were determined at various time points. Since no difference was observed for Atf3 and Ddit3 mRNA expression levels for early (2 h) and late (24 h) control cultures, values we pooled and statistically compared versus treatment groups. As shown in Fig. 2b, expression levels of Atf3 mRNA were increased as early as 2 h after sodium azide application, peaked at 4 h and thereafter steadily declined till 24 h post application. Ddit3 showed a similar, yet shifted course of expression induction. Expression of Ddit3 mRNA was increased as early as 4 h after sodium azide application, peaked at 12 h and thereafter declined till 24 h post application.

Inhibition of the respiratory chain in cultured oligodendrocytes induces mitochondrial membrane depolarization and oxidative stress

To verify that inhibition of the respiratory chain indeed blocks mitochondrial activity, we measured mitochondrial membrane potential (DΨm) after sodium azide treatment, which is critical for maintaining the physiological function of the respiratory chain to generate ATP. As shown in Fig. 3, numbers of depolarized cells after 1 h sodium azide treatment were significantly higher compared to control cultures.

Next, we verified that inhibition of the respiratory chain results in oxidative stress in cultured oligodendrocytes. To this end, OLN93 cells were treated for 1 h with the different inhibitors, and levels of ROS were quantified via flow cytometry based on the intracellular detection of superoxide radicals. As shown in Fig. 4, intracellular superoxide radical levels were significantly increased in rotenone (+193 ! 4%), antimycin (+267 ! 7%), sodium azide (+162 ! 11%), and oligomycin (+176 ! 6%) treated cultures. No accumulation of superoxide radical levels was observed in tunicamycin-

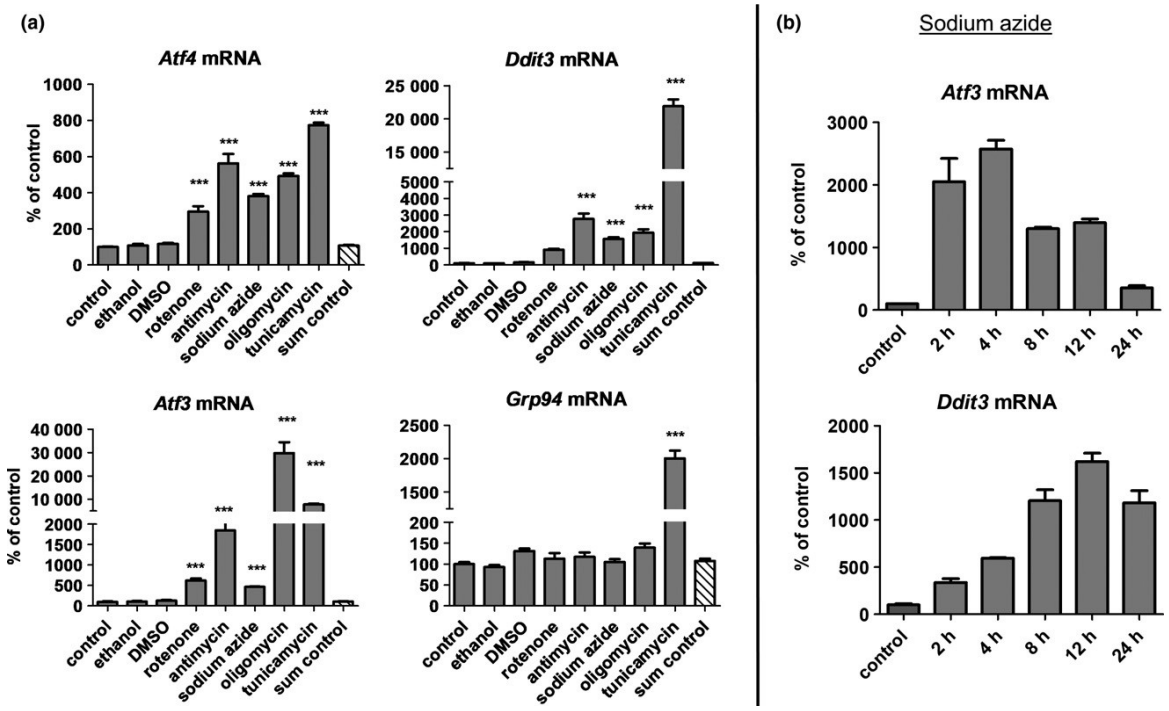

Fig. 2 Chemical hypoxia induces the expression of key integrated stress response transcription factors. (a) Atf3, Atf4, Ddit3, and Grp94 mRNA expression in OLN93 cells, stressed with different respiratory chain inhibitors and the N-linked glycosylation inhibitor tunicamycin. The following concentrations were used: rotenone (1 lM), antimycin (10 lM), sodium azide (10 mM), oligomycin (10 lM), tunicamycin (50 lg/mL). Comparison of expression levels between control (10 culture wells; one representative experiment) and treated cultures (at least four culture wells; one representative experiment) was done using one-way ANOVA with the obtained p-values corrected for multiple testing using the Dunnett's post hoc test. Significant differences with respect to control cultures are indicated by *$p < 0.05$, **$p < 0.01$, or ***$p < 0.001$. (b) Ddit3 and Atf3 mRNA expression in OLN93 cells, stressed for different periods with the complex-IV inhibitor sodium azide (10 mM; at least three culture wells; one representative experiment). Note the different scaling of the y-axis.

exposed cultures (data not shown). These results suggest that accumulation of intracellular ROS might result in the induction of ISR elements in oligodendrocytes.

Atf3 and Ddit3 is induced in primary oligodendrocytes and an in vivoremyelination model

Next, we wanted to know whether Atf3 and Ddit3 induction is an artifact of the applied oligodendrocyte cell line, or relevant for the in vivo situation. To this end, primary rat oligodendrocyte cultures were treated with sodium azide for 24 h and Atf3 and Ddit3 mRNA expression levels were determined by RT rt-PCR. As shown in Fig. 5a, Ddit3 mRNA expression was induced by sodium azide (+309 ! 28%), and to a higher extent by tunicamycin (+1306 ! 115%). A comparable expression induction was observed for Atf3 mRNA (sodium azide +471 ! 56%; tunicamycin +1438 ! 156%). Second, male C57Bl6 mice were intoxicated for 5 weeks with the copper chelator cuprizone (Kipp et al. 2009), and DDIT3 protein expression was analyzed by immunofluorescence staining. After a 5-week cuprizone intoxication period, early remyelination is ongoing, as shown by several groups (Kipp et al. 2009; Slowik et al. 2015). In line with previous reports, the midline of the corpus callosum was severely demyelinated after 5 weeks of cuprizone intoxication (see Fig. 5b). At this time point, numbers of APC$^+$ (767 ! 70.0 cells/mm^2) oligodendrocytes were low, but high numbers of OLIG2$^+$ cells (1346 ! 86.5 cells/mm^2) were found in the midline of the corpus callosum, indicating early remyelination. As shown in Fig. 5c, numerous OLIG2$^+$ cells expressed DDIT3 during early remyelination.

Complex-IV inhibition induces eIF2a-phosphorylation and ATF4 induction

Oxidative stress has been shown to promote eIF2a phosphorylation in different cell lines (Rajesh et al. 2015). Beyond, an important property of PERK and p-eIF2a is the adaptation of cells to oxidative stress caused by ROS formation in the intracellular environment (Harding et al. 2003; Back et al. 2009). In a next step, we, therefore,

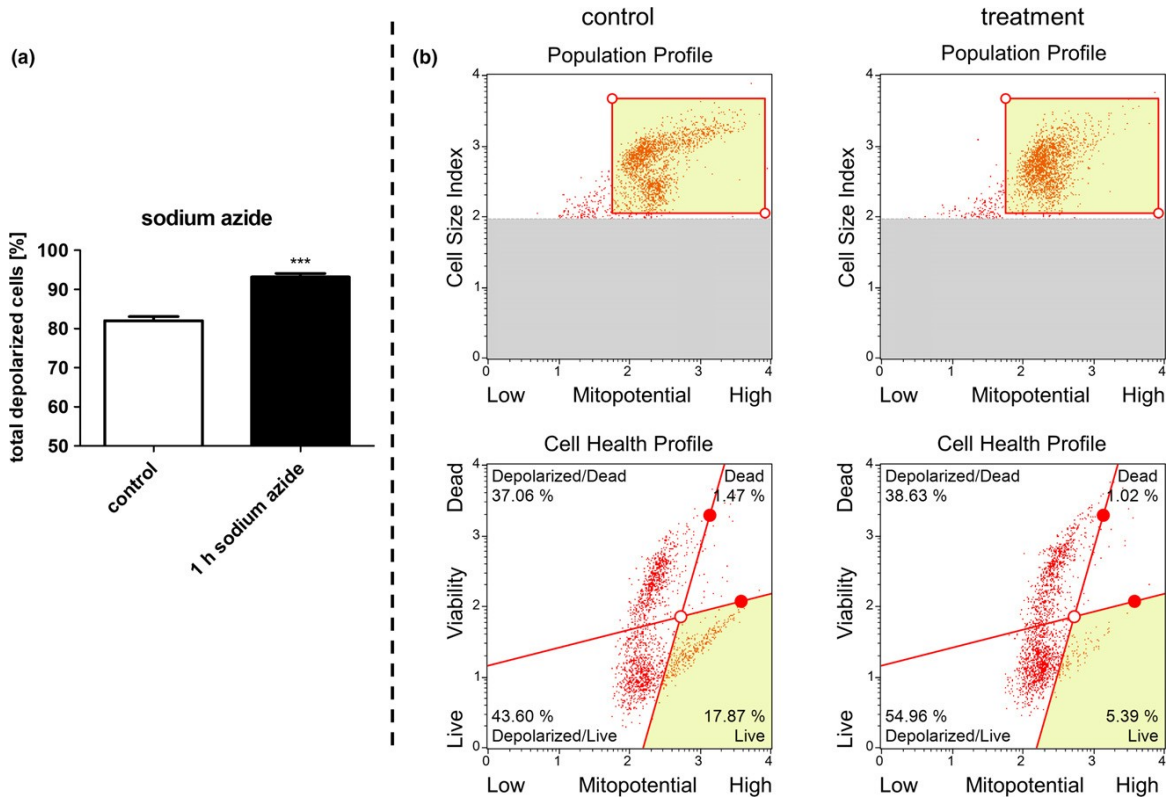

Fig. 3 Sodium azide treatment induces loss of mitochondrial membrane potential (DΨm). (a) Mitochondrial membrane potential in OLN93 cells after 1 h sodium azide (100 mM) exposure. Comparison of expression levels between control (six culture wells; one representative experiment) and treated cultures (three culture wells; one representative experiment) was done using t-test. Significant differences with respect to control cultures are indicated by *p < 0.05, **p < 0.01, or ***p < 0.001. (b) Representative illustration of the applied gating strategy. The upper plots show the threshold marker for eliminating debris based on cell size. The lower plots show the gated cells with four distinct cell populations: dead cells with a putative unspecific intact mitochondrial membrane potential (upper right); dead cells with a breakdown of the mitochondrial membrane potential (upper left); viable cells with an intact mitochondrial membrane potential (lower right); viable cells with a breakdown of the mitochondrial membrane potential (lower left). Note that in (a) the sum of viable and dead cells with a breakdown of the mitochondrial membrane potential was statistically compared. Thresholding was performed in a blinded manner and identical in control and treated cultures.

analyzed by western blotting experiments whether the PERK-eIF2a-ATF4 pathway is active in sodium azide-treated oligodendrocyte cultures. As demonstrated in Fig. 5 PERK phosphorylation was evident in thapsigargin (300 nM) (b), but not in sodium azide-exposed cultures ($p = 0.26$). In contrast, sodium azide did promote eIF2a phosphorylation ($p = 0.027$). Furthermore, higher ATF4 protein levels were observed in sodium azide-exposed OLN93 cells.

NRF2-activation induces ISR in oligodendrocytes

To investigate a possible causal relationship between oxidative stress and ISR induction, stable lentiviral-based gene silencing in OliNeu cells was performed to knockdown either Keap1 or Nrf2 expression. We have chosen OliNeu cells rather than OLN93 cells for these experiments because in our hands, a more stable transfection efficiency was obtained with this particular oligodendrocyte cell line. First, we verified efficacy of the applied siRNA protocol. As shown in Fig. 7a, Nrf2 mRNA expression levels were significantly reduced (!63%) in cultures exposed to Nrf2 but not to Keap1 targeting siRNA, respectively. The opposite was true for Keap1 mRNA expression, which was significantly reduced in cultures exposed to Keap1 (!62%), but not to Nrf2 targeting siRNA, respectively. Furthermore, we determined NRF2 protein levels by western blotting experiments. As shown in Fig. 7b, a profound reduction in NRF2 protein levels was observed in cultures exposed to Nrf2, but not to Keap1 targeting siRNA. After having verified sufficient transfection efficacy, we can assume that while in Keap1

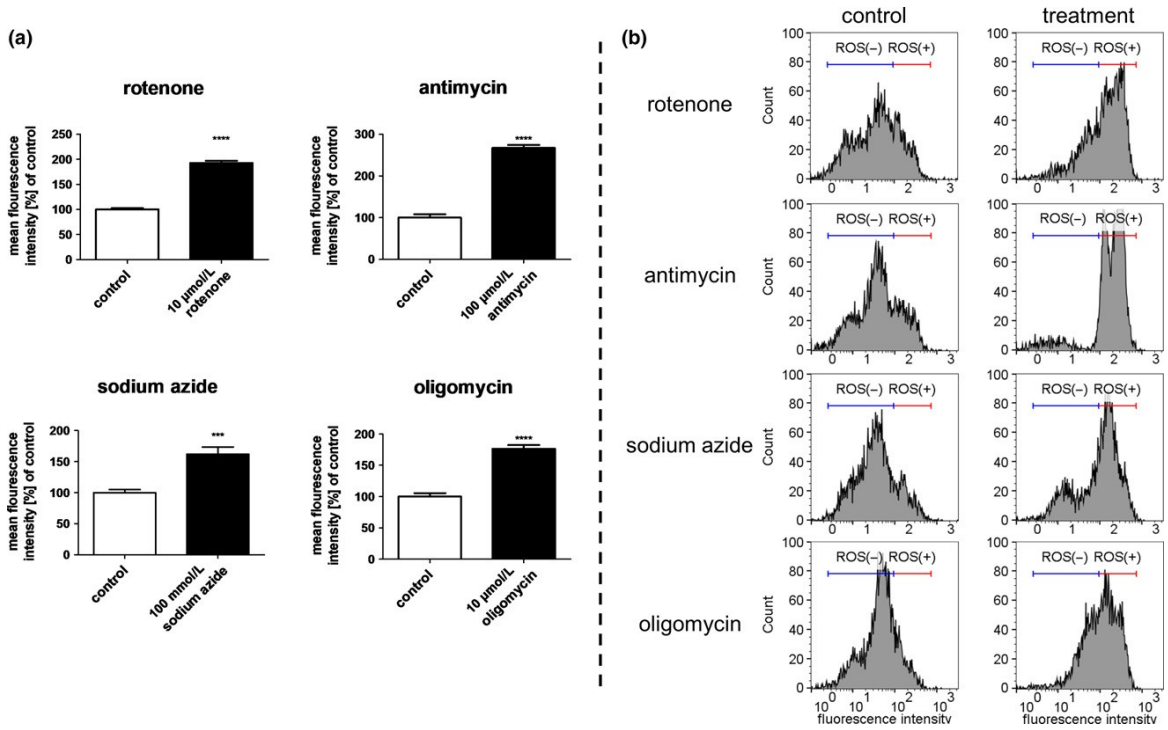

Fig. 4 Chemical hypoxia induces oxidative stress in OLN93 cells. (a) Mean fluorescence intensity after dihydroethidium staining in control (six biological replicates) and stressed oligodendrocytes (1 h; six culture wells; two independent experiments), determined by flow cytometry analysis. (b) Representative plots from Muse ! Oxidative Stress Assay. Plots show the histograms of gated cells with two markers providing data on two cell populations: reactive oxygen species (ROS !) and ROS + cells. Thresholding was performed in a blinded manner and identical in control and treated cultures. Comparison of fluorescence intensity levels between control and treated cultures was done using t-test. Significant differences with respect to control cultures are indicated by *p < 0.05, **p < 0.01, ***p < 0.001, or ****p < 0.0001. Six wells were included per treatment group.

cells, the NRF2-dependant cytoprotective machinery is constitutively activated, Nrf2$^{!/!}$ cells are insufficient to respond to cellular oxidative stress. Next, Keap1$^{!/!}$ Nrf2$^{!/!}$, and non-target transfected cells were treated with the complex-IV inhibitor sodium azide (24 h; 1 mM), and the mRNA expression of Atf3 and Ddit3 was analyzed by RT rt-PCR. As expected, Atf3 (+204 " 15%) and Ddit3 (+177 " 6%) expression were induced in sodium azide treated non-target transfected cells (Fig. 7c). The magnitude of Atf3 ($p < 0.01$) and Ddit3 ($p < 0.001$) mRNA expression was higher in Keap1$^{!/!}$ compared to non-target transfected cells. Of note, Atf3 ($p < 0.001$) and Ddit3 $p < 0.001$) expression induction was almost absent in Nrf2$^{!/!}$ versus non-target transfected cells.

Discussion

In this work, we demonstrated that inhibition of the respiratory chain at various levels induces oxidative stress in cultured oligodendrocytes which is paralleled by the expression induction of distinct ISR members, namely Atf3, Atf4, and Ddit3. Atf3 and Ddit3 expression induction is potentiated in Keap1$^{!/!}$ cells and absent in cells lacking the oxidative stress-related transcription factor NRF2. Even though regulation of the ISR components were not verified on the protein level in this study, our results provide strong evidence that oxidative stress in oligodendrocytes activates an endoplasmic reticulum stress response in a NRF2-dependent manner and, in consequence, might regulate oligodendrocyte degeneration in MS and other neurological disorders.

Mitochondria produce ATP (adenosine triphosphate) through the process of respiration and oxidative phosphorylation thereby acting as the primary source of energy in almost all cells. The process of oxidative phosphorylation involves coupling of both redox and phosphorylation reactions in the inner membrane of mitochondria resulting in effective ATP synthesis. During this process, electrons from NADH (nicotinamide adenine dinucleotide) or FADH2 (flavin adenine dinucleotide) are transported

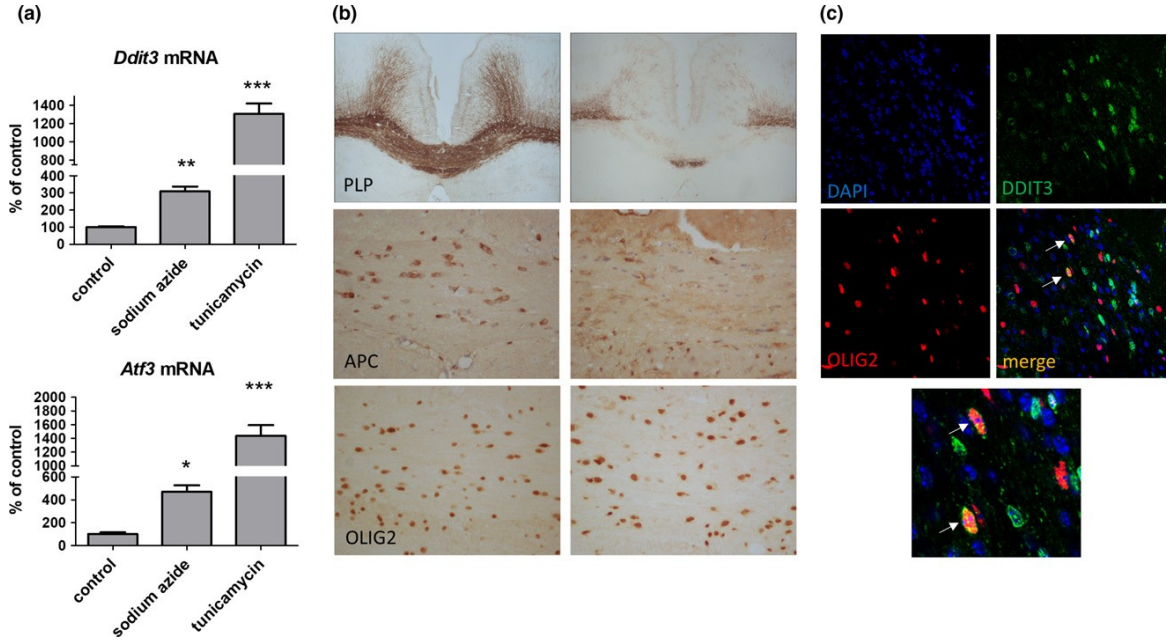

Fig. 5 Oligodendrocyte progenitor cells express DDIT3 and ATF3 in vitro and in vivo. (a) Ddit3 and Atf3 mRNA expression in primary rat oligodendrocyte cultures stressed with the respiratory chain inhibitor sodium azide or the N-linked glycosylation inhibitor tunicamycin. The following concentrations were used: sodium azide (10 mM), tunicamycin (25 lg/mL). Comparison of expression levels between control (five culture wells; one independent experiment) and treated cultures (five culture wells; one independent experiment) was done using Welch's t-test. Significant differences with respect to control cultures are indicated by $*p < 0.05$, $**p < 0.01$, or $***p < 0.001$. (b) Demyelination [anti- proteolipid protein (PLP)], loss of mature oligodendrocytes (anti-APC), but accumulation of oligodendrocyte progenitor cells (anti-OLIG2) in the midline of the corpus callosum after acute cuprizone-induced demyelination (5 weeks cuprizone; 0.25%). (c) Immunofluorescence double-labeling to demonstrate DDIT3 expression in OLIG2$^+$ oligodendrocyte progenitor cells (five animals per group; one independent experiment).

through the electron transport chain, comprising of complexes I–IV, to create a proton gradient across the inner mitochondrial membrane (Fig. 8). The consequent movement of protons from the mitochondrial matrix to the intermembrane space creates an electrochemical gradient. This electrochemical gradient consists of a pH gradient (DpH) and an electrical gradient (Dw) that drives the synthesis of ATP from ADP (adenosine diphosphate) through the enzyme ATP synthase (complex-V). As shown in Fig. 3, treatment of cultures with sodium azide induces a rapid breakdown of the mitochondrial inner transmembrane potential, showing that the applied sodium azide concentration indeed impairs oxidative phosphorylation in OLN93 cells. Interestingly, we observed the same in oligodendrocytes cultured in human liquor (unpublished observation), strongly suggesting that this is not an effect because of the applied culture conditions. Although we have not tested the electrochemical gradient across the mitochondrial membrane in cultures exposed to the other respiratory chain blockers (i.e., rotenone, antimycin, or oligomycin), one should anticipate, based on published work (Kalbacova et al. 2003; Moon et al. 2005; Han et al. 2008), that all four blockers induce mitochondrial membrane depolarization. Mitochondrial membrane potential changes have been implicated in apoptosis, necrotic cell death, and caspase-independent cell death processes (Gilissen et al. 2017; Liao et al. 2017). Depolarization of the inner mitochondrial membrane potential is, thus, a reliable indicator of mitochondrial dysfunction.

It is well known that mitochondria are the major sites for generation of ROS in cells. Since the respiratory chain is 'leaky', electrons can escape from the respiratory chain and reduce O_2, resulting in the generation of superoxide, the primary ROS. As shown in Fig. 4, the inhibition of the respiratory chain resulted in a robust accumulation of superoxide radicals under the applied culture conditions. How exactly respiratory chain inhibition results in oxidative stress in not known but alpha-ketoglutarate dehydrogenase might be involved in this process. Alpha-ketoglutarate dehydrogenase represents a key Krebs cycle enzyme and is also able to produce ROS (Starkov et al. 2004). ROS formation by alpha-ketoglutarate dehydrogenase is regulated by the NADH/NAD+ ratio, suggesting that this enzyme could substantially contribute to generation of oxidative

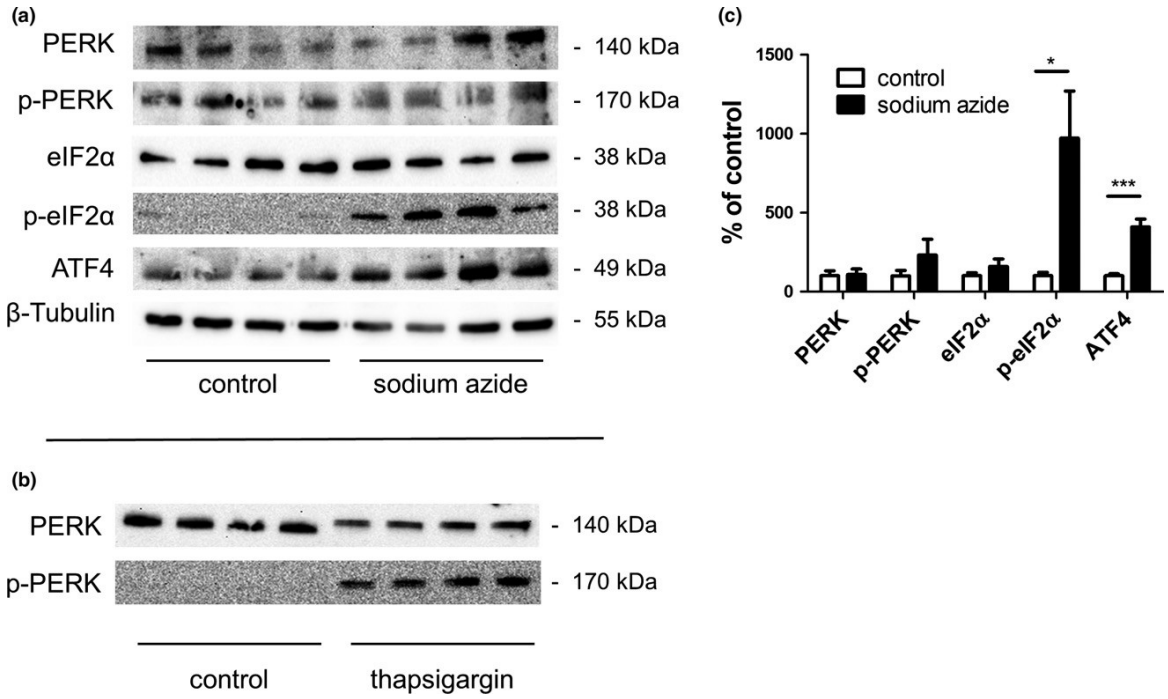

Fig. 6 Chemical hypoxia-induced integrated stress response (ISR) activation. (a) Representative western blot of sodium azide-treated (2 h; 100 mM) OLN93 cells. (b) Representative western blot of thapsigargin-treated (2 h; 300 nM) OLN93 cells. (c) Semi-quantification of western blot experiments (five culture wells; one representative experiment) by densitometrical analyses. Phosphorylated-PERK (p-PERK) and phosphorylated eIF2a (p-eIF2a) levels were semi-quantified relative to entire PERK or eIF2a-levels, respectively. ATF4, non-phosphorylated PERK, and non-phosphorylated eIF2a protein levels were semi-quantified relative to ß-tubulin concentrations. The ratio of phosphorylated eIF2a/PERK relative to total eIF2a/PERK was determined by densitometry and was set to 100 in untreated cells. Comparison of protein expression levels between different groups was done using t-test. Significant differences with respect to control cultures are indicated by *p < 0.05, **p < 0.01, or ***p < 0.001. Note the absence of PERK phosphorylation, but presence of eIF2a phosphorylation, paralleled by increased ATF4 protein levels in sodium azide-exposed cultures.

stress because of inhibition of the respiratory chain and subsequent NADH accumulation within the mitochondrial matrix. Of note, increased ROS levels were not observed in OLN93 cells stressed by tunicamycin (data not shown), which inhibits protein N-glycosylation, showing that accumulation of ROS is not because of ER stress but rather as a result of mitochondrial deficiency.

ROS accumulation was paralleled by the robust induction of well-known ISR marker genes, namely Atf3, Atf4, and Ddit3. The fact that states of oxidative stress can activate the ISR is not new. For example, it has been shown that under conditions of moderate hypoxia, ROS induce the ISR, thereby promoting energy and redox homeostasis and enhancing cellular survival of mouse embryonic fibroblasts (Liu et al. 2008). Comparably, exposure of human diploid fibroblasts or HeLa cells to hypoxia led to phosphorylation of eIF2a and ATF4 induction in a PERK-dependent manner (Koumenis et al. 2002; Blais et al. 2004). Increase in Ddit3 expression during experimental hypoxia has as well been reported to occur, for example, in mouse islets cells (Bensellam et al. 2016) and cardiomyocytes (Gao et al. 2016). This is, however, to the best of our knowledge, the first report showing ISR induction caused by 'chemical hypoxia', and linking this induction to the KEAP1/NRF2 pathway. Since NRF2 is a direct PERK substrate, and NRF2 nuclear translocation is independent of eIF2a phosphorylation (Cullinan et al. 2003), future studies have to show whether NRF2 directly regulates Atf3, At4, and Ddit3 expression. Indeed, it has been suggested that PERK signaling, via activation of the NRF2 and ATF4 transcription factors, coordinates the convergence of ER stress with oxidative stress signaling (Cullinan and Diehl 2006). Furthermore, it has been show that NRF2 transcriptionally up-regulates Atf3 expression in astrocytes (Kim et al. 2010).

During hypoxia, there is an elevation in reducing equivalents (mostly NADH and FADH2) that build up, particularly in the mitochondria, when insufficient O_2 is available for reduction by the electron transport chain. This buildup of reducing equivalents also makes electrons more available for

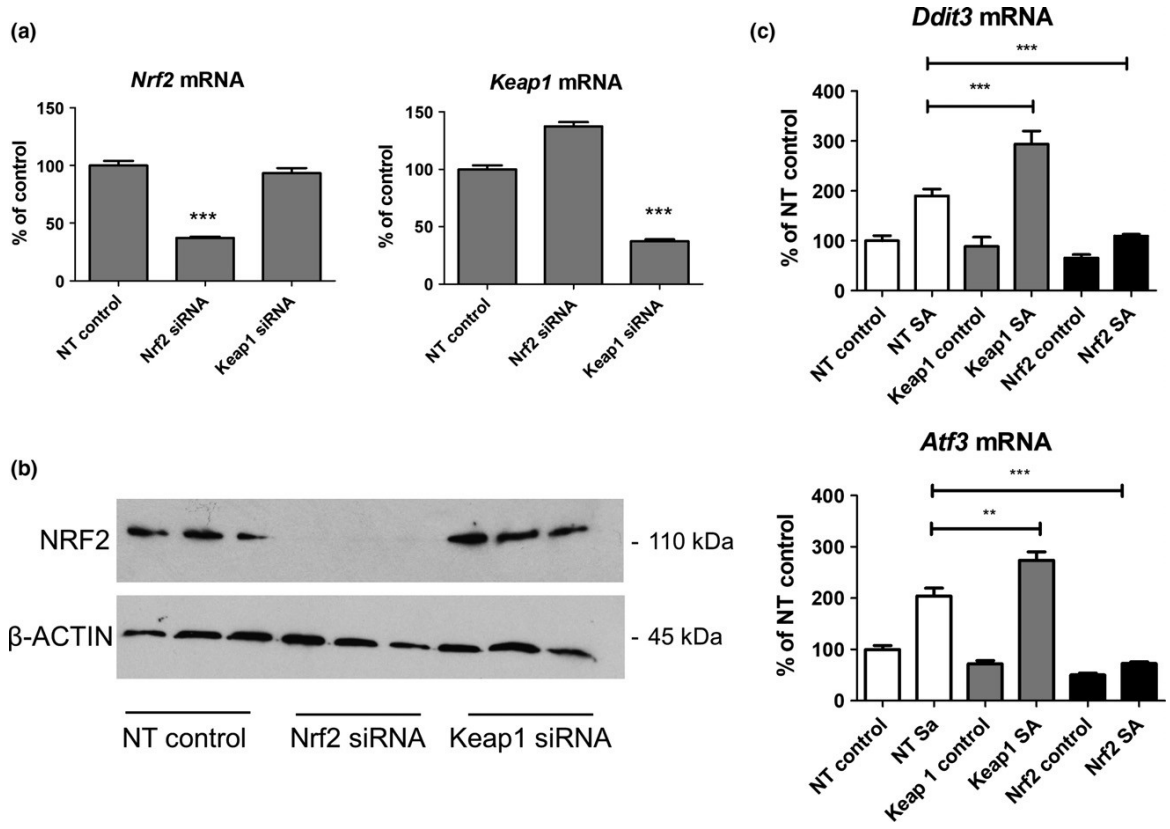

Fig. 7 Chemical hypoxia-induced integrated stress response (ISR) activation is NRF2-dependant. (a) Nrf2 and Keap1 mRNA expression in non-template transfected (NT-control), Nrf2 targeting siRNA (Nrf2 siRNA), and Keap1 targeting siRNA (Keap1 siRNA) transfected OliNeu cells. Comparison of gene expression levels between different groups (four culture wells; one independent experiment) was done using Welch's t-test. Significant differences with respect to control cultures are indicated by *p < 0.05, **p < 0.01, or ***p < 0.001. (b) Representative western blot to demonstrate reduction in NRF2 protein levels in transfected OliNeu cells. ß-ACTIN levels were used as internal loading control. (c) Ddit3 and Atf3 mRNA expression levels after treatment with the complex-IV inhibitor sodium azide (24 h; 1 mM) in the murine oligodendrocyte cell line OliNeu, in which Nrf2 or Keap1 gene expression was silenced by lentiviral shRNA delivery. Comparison of gene expression levels between different groups (12 culture wells; two independent experiments) was done using t-test. Significant differences with respect to control cultures are indicated by *p < 0.05, **p < 0.01, or ***p < 0.001. Abbreviations: NT (non -target), SA (sodium azide).

reduction reactions such as the reduction of O_2 to superoxide. By this mechanism, tissue hypoxia might lead to ROS accumulation and in consequence ISR induction. ROS accumulation can as well be caused by 'chemical hypoxia' which results from poisoning of the electron transport system as done in this study. Both, chemical hypoxia and tissue hypoxia, lead to elevations in reducing equivalents but in chemical hypoxia, sufficient O_2 is presumably always available for reduction, whereas in tissue hypoxia, as one approaches anoxia, oxygen availability can become a critical substrate for production of ROS. Thus, chemical hypoxia might result in higher ROS levels compared to tissue hypoxia and thus be very potent in ISR induction. In this context, the term 'virtual hypoxia' is of particular interest (Trapp and Stys 2009). Pathological studies using MS tissues have implicated reactive oxygen and nitrogen species in lesion formation and have suggested that such agents may impair mitochondrial metabolism, resulting in a tissue energy deficiency (Aboul-Enein and Lassmann 2005). Thus, virtual hypoxia might induce massive ROS accumulation and in consequence ISR activation in MS tissues. Notably, ER stress markers are expressed in inflammatory MS lesions (Mhaille et al. 2008; Cunnea et al. 2011), in experimental autoimmune encephalomyelitis (Lin et al. 2007) and the cuprizone model (Goldberg et al. 2013), both preclinical animal models for MS.

One of the factors induced by mitochondrial chain inhibition is the transcription factor DDIT3 which is classically regarded pro-apoptotic. Studies using Ddit3$^{-/-}$ mice have established the role of DDIT3 during stress-

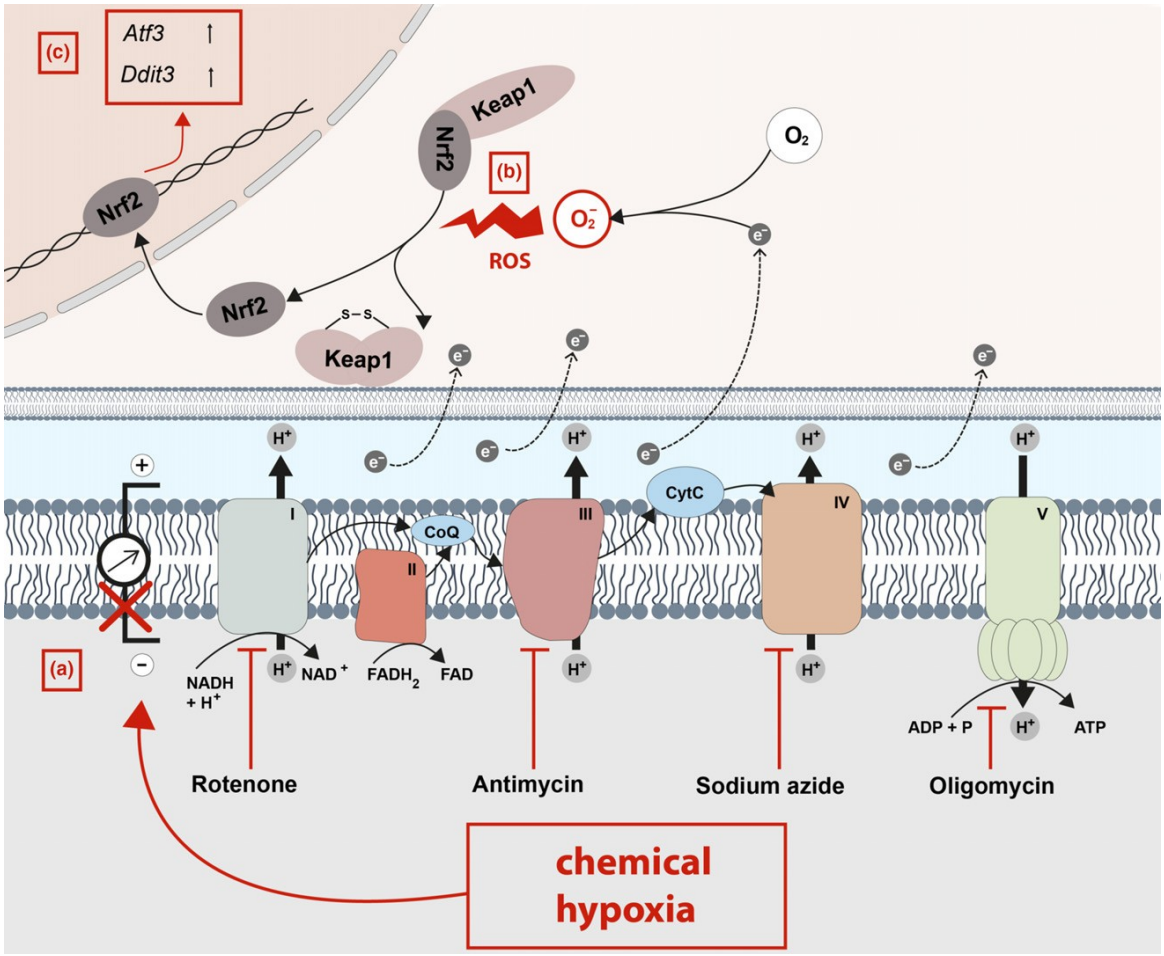

Fig. 8 Chemical hypoxia – mode of action. Chemical hypoxia induces loss of mitochondrial membrane potential (DΨm) (a). 'Leaky' electrons can escape from the respiratory chain and reduce O_2, resulting in the generation of superoxide, the primary ROS (b). As a consequence, NRF2 is released from KEAP1 and translocates into the nucleus where it binds to the antioxidant response element (ARE), thereby activating the transcription of Atf3 and Ddit3 (C).

induced apoptosis in a number of disease models including renal dysfunction (Zinszner et al. 1998), diabetes (Song et al. 2008), ethanol-induced hepatocyte injury (Ji et al. 2005), experimental colitis (Namba et al. 2009), advanced atherosclerosis (Thorp et al. 2009), and cardiac-pressure overload (Fu et al. 2010). Furthermore, there is strong evidence that DDIT3 regulates cell death in neurodegenerative and neuroinflammatory disorders including Parkinson's disease (Silva et al. 2005), subarachnoid hemorrhage (He et al. 2012), Alzheimer's disease (Prasanthi et al. 2011), multiple system atrophy (Makioka et al. 2010), and spinal cord injury (Ohri et al. 2011). However, the relevance of DDIT3 for survival of myelinating cells (i.e., oligodendrocytes and Schwann cells) is controversially discussed. On one hand, deleting the Ddit3 gene in a model for Pelizaeus–Merzbacher disease reduces lifespan and increases cell death indicating that DDIT3 or its targets are adaptive and act as pro-survival factors (Southwood et al. 2002). On the other hand, ablation of Ddit3 in a model for Charcot–Marie–Tooth disease type 1B completely rescues motor deficits and ameliorates active demyelination (D'Antonio et al. 2013) indicating that in Schwann cells, DDIT3 is indeed pro-apoptotic. In experimental autoimmune encephalomyelitis, one of the most commonly used MS animal models, the role of DDIT3 appears to be redundant (Deslauriers et al. 2011). These contrasting results suggest that the role of DDIT3 in myelinating cells is strongly context dependent. While we have not investigated whether DDIT3 induction regulates oligodendrocyte injury in this in vitro model, a recent study from our group showed that metabolic oligodendrocyte degeneration in a MS animal model is paralleled by

oxidative injury, and that hyperactivation of the NRF2/ARE system (via Keap1 knockdown) ameliorates oligodendrocyte degeneration and in consequence demyelination (Draheim et al. 2016). In the very same model, stressed oligodendrocytes clearly demonstrate ISR activation (Goldberg et al. 2013). It would now be interesting to show whether Ddit3$^{-/-}$ mice (Zinszner et al. 1998) are protected from cuprizone-induced oligodendrocyte apoptosis.

In summary, this study provides strong evidence that oxidative stress in oligodendrocytes activates an ISR and in consequence might regulate oligodendrocyte degeneration in MS and other neurological disorders.

Acknowledgments and conflict of interest disclosure

This study was supported by the Dr Robert Pfleger Stiftung (M.K.) and the Deutsche Forschungsgemeinschaft (KI 1469/8-1). The technical support from S. Wegbel is acknowledged. The fruitful discussion with Dr Fabian Baertling (Department of General Pediatrics, Duesseldorf, Germany) is highly appreciated. We thank Christiane Richter-Landsberg (Oldenburg, Germany) for providing OLN93 cells, and Jacqueline Trotter (Mainz, Germany) for providing OliNeu cells. We state that this study was not pre-registered. The authors declare no competing financial interests.

All experiments were conducted in compliance with the ARRIVE guidelines.

References

Aboul-Enein F. and Lassmann H. (2005) Mitochondrial damage and histotoxic hypoxia: a pathway of tissue injury in inflammatory brain disease? Acta Neuropathol. 109, 49–55.

Back S. H., Scheuner D., Han J., Song B., Ribick M., Wang J., Gildersleeve R. D., Pennathur S. and Kaufman R. J. (2009) Translation attenuation through eIF2alpha phosphorylation prevents oxidative stress and maintains the differentiated state in beta cells. Cell Metab. 10, 13–26.

Barnett M. H. and Prineas J. W. (2004) Relapsing and remitting multiple sclerosis: pathology of the newly forming lesion. Ann. Neurol. 55, 458–468.

Bensellam M., Maxwell E. L., Chan J. Y., Luzuriaga J., West P. K., Jonas J. C., Gunton J. E. and Laybutt D. R. (2016) Hypoxia reduces ER-to-Golgi protein trafficking and increases cell death by inhibiting the adaptive unfolded protein response in mouse beta cells. Diabetologia 59, 1492–1502.

Blais J. D., Filipenko V., Bi M., Harding H. P., Ron D., Koumenis C., Wouters B. G. and Bell J. C. (2004) Activating transcription factor 4 is translationally regulated by hypoxic stress. Mol. Cell. Biol. 24, 7469–7482.

Bramow S., Frischer J. M., Lassmann H., Koch-Henriksen N., Lucchinetti C. F., Sorensen P. S. and Laursen H. (2010) Demyelination versus remyelination in progressive multiple sclerosis. Brain 133, 2983–2998.

Bruce C. C., Zhao C. and Franklin R. J. (2010) Remyelination -An effective means of neuroprotection? Horm. Behav. 57, 56–62.

Cao S. S. and Kaufman R. J. (2014) Endoplasmic reticulum stress and oxidative stress in cell fate decision and human disease. Antioxid. Redox Signal. 21, 396–413.

Chang A., Nishiyama A., Peterson J., Prineas J. and Trapp B. D. (2000) NG2-positive oligodendrocyte progenitor cells in adult human brain and multiple sclerosis lesions. J. Neurosci. 20, 6404–6412.

Chang A., Tourtellotte W. W., Rudick R. and Trapp B. D. (2002) Premyelinating oligodendrocytes in chronic lesions of multiple sclerosis. N. Engl. J. Med. 346, 165–173.

Clarner T., Parabucki A., Beyer C. and Kipp M. (2011) Corticosteroids impair remyelination in the corpus callosum of cuprizone-treated mice. J. Neuroendocrinol. 23, 601–611.

Cui Q. L., Kuhlmann T., Miron V. E., Leong S. Y., Fang J., Gris P., Kennedy T. E., Almazan G. and Antel J. (2013) Oligodendrocyte progenitor cell susceptibility to injury in multiple sclerosis. Am. J. Pathol. 183, 516–525.

Cullinan S. B. and Diehl J. A. (2006) Coordination of ER and oxidative stress signaling: the PERK/Nrf2 signaling pathway. Int. J. Biochem. Cell Biol. 38, 317–332.

Cullinan S. B., Zhang D., Hannink M., Arvisais E., Kaufman R. J. and Diehl J. A. (2003) Nrf2 is a direct PERK substrate and effector of PERK-dependent cell survival. Mol. Cell. Biol. 23, 7198–7209.

Cunnea P., Mhaille A. N., McQuaid S., Farrell M., McMahon J. and FitzGerald U. (2011) Expression profiles of endoplasmic reticulum stress-related molecules in demyelinating lesions and multiple sclerosis. Mult. Scler. 17, 808–818.

D'Antonio M., Musner N., Scapin C., Ungaro D., Del Carro U., Ron D., Feltri M. L. and Wrabetz L. (2013) Resetting translational homeostasis restores myelination in Charcot-Marie-Tooth disease type 1B mice. J. Exp. Med. 210, 821–838.

Deslauriers A. M., Afkhami-Goli A., Paul A. M., Bhat R. K., Acharjee S., Ellestad K. K., Noorbakhsh F., Michalak M. and Power C. (2011) Neuroinflammation and endoplasmic reticulum stress are coregulated by crocin to prevent demyelination and neurodegeneration. J. Immunol. (Baltimore, Md.: 1950), 187, 4788–4799.

Dincman T. A., Beare J. E., Ohri S. S., Gallo V., Hetman M. and Whittemore S. R. (2016) Histone deacetylase inhibition is cytotoxic to oligodendrocyte precursor cells in vitro and in vivo. Int. J. Dev. Neurosci. 54, 53–61.

Draheim T., Liessem A., Scheld M. et al. (2016) Activation of the astrocytic Nrf2/ARE system ameliorates the formation of demyelinating lesions in a multiple sclerosis animal model. Glia 64, 2219–2230.

Edagawa M., Kawauchi J., Hirata M., Goshima H., Inoue M., Okamoto T., Murakami A., Maehara Y. and Kitajima S. (2014) Role of activating transcription factor 3 (ATF3) in endoplasmic reticulum (ER) stress-induced sensitization of p53-deficient human colon cancer cells to tumor necrosis factor (TNF)-related apoptosis-inducing ligand (TRAIL)-mediated apoptosis through up-regulation of death receptor 5 (DR5) by zerumbone and celecoxib. J. Biol. Chem. 289, 21544–21561.

Fern R. F., Matute C. and Stys P. K. (2014) White matter injury: Ischemic and nonischemic. Glia 62, 1780–1789.

Fu H. Y., Okada K., Liao Y. et al. (2010) Ablation of C/EBP homologous protein attenuates endoplasmic reticulum-mediated apoptosis and cardiac dysfunction induced by pressure overload. Circulation 122, 361–369.

Funfschilling U., Supplie L. M., Mahad D. et al. (2012) Glycolytic oligodendrocytes maintain myelin and long-term axonal integrity. Nature 485, 517–521.

Gao Y., Jia P., Shu W. and Jia D. (2016) The protective effect of lycopene on hypoxia/reoxygenation-induced endoplasmic reticulum stress in H9C2 cardiomyocytes. Eur. J. Pharmacol. 774, 71–79.

Gill A., Gao N. and Lehrman M. A. (2002) Rapid activation of glycogen phosphorylase by the endoplasmic reticulum unfolded protein response. J. Biol. Chem. 277, 44747–44753.

Gillissen B., Richter A., Richter A., Preissner R., Schulze-Osthoff K., Essmann F. and Daniel P. T. (2017) Bax/Bak-independent mitochondrial depolarization and reactive oxygen species induction by sorafenib overcome resistance to apoptosis in renal cell carcinoma. J. Biol. Chem. 292, 6478–6492.

Goldberg J., Daniel M., van Heuvel Y., Victor M., Beyer C., Clarner T. and Kipp M. (2013) Short-term cuprizone feeding induces selective amino acid deprivation with concomitant activation of an integrated stress response in oligodendrocytes. Cell. Mol. Neurobiol. 33, 1087–1098.

Haider L., Fischer M. T., Frischer J. M. et al. (2011) Oxidative damage in multiple sclerosis lesions. Brain 134, 1914–1924.

Han Y. H., Kim S. H., Kim S. Z. and Park W. H. (2008) Antimycin A as a mitochondrial electron transport inhibitor prevents the growth of human lung cancer A549 cells. Oncol. Rep. 20, 689–693.

Harding H. P., Zhang Y., Zeng H. et al. (2003) An integrated stress response regulates amino acid metabolism and resistance to oxidative stress. Mol. Cell 11, 619–633.

He Z., Ostrowski R. P., Sun X., Ma Q., Huang B., Zhan Y. and Zhang J. H. (2012) CHOP silencing reduces acute brain injury in the rat model of subarachnoid hemorrhage. Stroke 43, 484–490.

Honmou O., Felts P. A., Waxman S. G. and Kocsis J. D. (1996) Restoration of normal conduction properties in demyelinated spinal cord axons in the adult rat by transplantation of exogenous Schwann cells. J. Neurosci. 16, 3199–3208.

Itoh K., Wakabayashi N., Katoh Y., Ishii T., O'Connor T. and Yamamoto M. (2003) Keap1 regulates both cytoplasmic-nuclear shuttling and degradation of Nrf2 in response to electrophiles. Genes Cells 8, 379–391.

Ji C., Mehrian-Shai R., Chan C., Hsu Y. H. and Kaplowitz N. (2005) Role of CHOP in hepatic apoptosis in the murine model of intragastric ethanol feeding. Alcohol. Clin. Exp. Res. 29, 1496–1503.

Kalbacova M., Vrbacky M., Drahota Z. and Melkova Z. (2003) Comparison of the effect of mitochondrial inhibitors on mitochondrial membrane potential in two different cell lines using flow cytometry and spectrofluorometry. Cytometry A 52, 110–116.

Kim K. H., Jeong J. Y., Surh Y. J. and Kim K. W. (2010) Expression of stress-response ATF3 is mediated by Nrf2 in astrocytes. Nucleic Acids Res. 38, 48–59.

Kipp M., Clarner T., Dang J., Copray S. and Beyer C. (2009) The cuprizone animal model: new insights into an old story. Acta Neuropathol. 118, 723–736.

Kipp M., Nyamoya S., Hochstrasser T. and Amor S. (2017) Multiple sclerosis animal models: a clinical and histopathological perspective. Brain Pathol. 27, 123–137.

Koumenis C., Naczki C., Koritzinsky M., Rastani S., Diehl A., Sonenberg N., Koromilas A. and Wouters B. G. (2002) Regulation of protein synthesis by hypoxia via activation of the endoplasmic reticulum kinase PERK and phosphorylation of the translation initiation factor eIF2alpha. Mol. Cell. Biol. 22, 7405–7416.

Kozutsumi Y., Segal M., Normington K., Gething M. J. and Sambrook J. (1988) The presence of malfolded proteins in the endoplasmic reticulum signals the induction of glucose-regulated proteins. Nature 332, 462–464.

Li G. L., Farooque M., Holtz A. and Olsson Y. (1999) Apoptosis of oligodendrocytes occurs for long distances away from the primary injury after compression trauma to rat spinal cord. Acta Neuropathol. 98, 473–480.

Liao H. Y., Kao C. M., Yao C. L., Chiu P. W., Yao C. C. and Chen S. C. (2017) 2,4,6-trinitrotoluene induces apoptosis via ROS-regulated mitochondrial dysfunction and endoplasmic reticulum stress in HepG2 and Hep3B cells. Sci. Rep. 7, 8148.

Lin W., Bailey S. L., Ho H., Harding H. P., Ron D., Miller S. D. and Popko B. (2007) The integrated stress response prevents demyelination by protecting oligodendrocytes against immune-mediated damage. J. Clin. Investig. 117, 448–456.

Liu B. and Li Z. (2008) Endoplasmic reticulum HSP90b1 (gp96, grp94) optimizes B-cell function via chaperoning integrin and TLR but not immunoglobulin. Blood 112, 1223–1230.

Liu L., Wise D. R., Diehl J. A. and Simon M. C. (2008) Hypoxic reactive oxygen species regulate the integrated stress response and cell survival. J. Biol. Chem. 283, 31153–31162.

Liu B., Chen X., Wang Z. Q. and Tong W. M. (2014) DNA damage and oxidative injury are associated with hypomyelination in the corpus callosum of newborn Nbn (CNS-del) mice. J. Neurosci. Res. 92, 254–266.

Makioka K., Yamazaki T., Fujita Y., Takatama M., Nakazato Y. and Okamoto K. (2010) Involvement of endoplasmic reticulum stress defined by activated unfolded protein response in multiple system atrophy. J. Neurol. Sci. 297, 60–65.

Marciniak S. J., Yun C. Y., Oyadomari S., Novoa I., Zhang Y., Jungreis R., Nagata K., Harding H. P. and Ron D. (2004) CHOP induces death by promoting protein synthesis and oxidation in the stressed endoplasmic reticulum. Genes Dev. 18, 3066–3077.

Matute C., Alberdi E., Domercq M., Sanchez-Gomez M. V., Perez-Samartin A., Rodriguez-Antiguedad A. and Perez-Cerda F. (2007) Excitotoxic damage to white matter. J. Anat. 210, 693–702.

Maus F., Sakry D., Biname F. et al. (2015) The NG2 proteoglycan protects oligodendrocyte precursor cells against oxidative stress via interaction with OMI/HtrA2. PLoS ONE 10, e0137311.

Mhaille A. N., McQuaid S., Windebank A., Cunnea P., McMahon J., Samali A. and FitzGerald U. (2008) Increased expression of endoplasmic reticulum stress-related signaling pathway molecules in multiple sclerosis lesions. J. Neuropathol. Exp. Neurol. 67, 200–211.

Moon Y., Lee K. H., Park J. H., Geum D. and Kim K. (2005) Mitochondrial membrane depolarization and the selective death of dopaminergic neurons by rotenone: protective effect of coenzyme Q10. J. Neurochem. 93, 1199–1208.

Moore S., Khalaj A. J., Yoon J. et al. (2013) Therapeutic laquinimod treatment decreases inflammation, initiates axon remyelination, and improves motor deficit in a mouse model of multiple sclerosis. Brain Behav. 3, 664–682.

Moore C. S., Cui Q. L., Warsi N. M., Durafourt B. A., Zorko N., Owen D. R., Antel J. P. and Bar-Or A. (2015) Direct and indirect effects of immune and central nervous system-resident cells on human oligodendrocyte progenitor cell differentiation. J. Immunol. (Baltimore, Md.: 1950), 194, 761–772.

Namba T., Tanaka K., Ito Y., Ishihara T., Hoshino T., Gotoh T., Endo M., Sato K. and Mizushima T. (2009) Positive role of CCAAT/enhancer-binding protein homologous protein, a transcription factor involved in the endoplasmic reticulum stress response in the development of colitis. Am. J. Pathol. 174, 1786–1798.

Natarajan C., Yao S. Y., Zhang F. and Sriram S. (2013) Activation of NOD2/RIPK2 pathway induces mitochondrial injury to oligodendrocyte precursor cells in vitro and CNS demyelination in vivo. J. Neuroimmunol. 265, 51–60.

Ohl K., Tenbrock K. and Kipp M. (2016) Oxidative stress in multiple sclerosis: central and peripheral mode of action. Exp. Neurol. 277, 58–67.

Ohri S. S., Maddie M. A., Zhao Y., Qiu M. S., Hetman M. and Whittemore S. R. (2011) Attenuating the endoplasmic reticulum stress response improves functional recovery after spinal cord injury. Glia 59, 1489–1502.

Pakos-Zebrucka K., Koryga I., Mnich K., Ljujic M., Samali A. and Gorman A. M. (2016) The integrated stress response. EMBO Rep. 17, 1374–1395.

Pantoni L., Garcia J. H. and Gutierrez J. A. (1996) Cerebral white matter is highly vulnerable to ischemia. Stroke, 27, 1641–1646; discussion 1647.

Patrikios P., Stadelmann C., Kutzelnigg A. et al. (2006) Remyelination is extensive in a subset of multiple sclerosis patients. Brain, 129, 3165–3172.

di Penta A., Moreno B., Reix S. et al. (2013) Oxidative stress and proinflammatory cytokines contribute to demyelination and axonal damage in a cerebellar culture model of neuroinflammation. PLoS ONE 8, e54722.

Pitt D., Werner P. and Raine C. S. (2000) Glutamate excitotoxicity in a model of multiple sclerosis. Nat. Med. 6, 67–70.

Prasanthi J. R., Larson T., Schommer J. and Ghribi O. (2011) Silencing GADD153/CHOP gene expression protects against Alzheimer's disease-like pathology induced by 27-hydroxycholesterol in rabbit hippocampus. PLoS ONE 6, e26420.

Prineas J. W. and Parratt J. D. (2012) Oligodendrocytes and the early multiple sclerosis lesion. Ann. Neurol. 72, 18–31.

Puthalakath H., O'Reilly L. A., Gunn P. et al. (2007) ER stress triggers apoptosis by activating BH3-only protein Bim. Cell 129, 1337–1349.

Rajesh K., Krishnamoorthy J., Kazimierczak U., Tenkerian C., Papadakis A. I., Wang S., Huang S. and Koromilas A. E. (2015) Phosphorylation of the translation initiation factor eIF2alpha at serine 51 determines the cell fate decisions of Akt in response to oxidative stress. Cell Death Dis. 6, e1591.

Richter-Landsberg C. and Heinrich M. (1996) OLN-93: a new permanent oligodendroglia cell line derived from primary rat brain glial cultures. J. Neurosci. Res. 45, 161–173.

Rosenzweig S. and Carmichael S. T. (2013) Age-dependent exacerbation of white matter stroke outcomes: a role for oxidative damage and inflammatory mediators. Stroke 44, 2579–2586.

Rutkowski D. T., Arnold S. M., Miller C. N. et al. (2006) Adaptation to ER stress is mediated by differential stabilities of pro-survival and pro-apoptotic mRNAs and proteins. PLoS Biol. 4, e374.

Santos C. X., Tanaka L. Y., Wosniak J. and Laurindo F. R. (2009) Mechanisms and implications of reactive oxygen species generation during the unfolded protein response: roles of endoplasmic reticulum oxidoreductases, mitochondrial electron transport, and NADPH oxidase. Antioxid. Redox Signal. 11, 2409–2427.

Schampel A., Volovitch O., Koeniger T. et al. (2017) Nimodipine fosters remyelination in a mouse model of multiple sclerosis and induces microglia-specific apoptosis. Proc. Natl Acad. Sci. USA 114, E3295–e3304.

Scheuer T., Brockmoller V., Blanco Knowlton M., Weitkamp J. H., Ruhwedel T., Mueller S., Endesfelder S., Buhrer C. and Schmitz T. (2015) Oligodendroglial maldevelopment in the cerebellum after postnatal hyperoxia and its prevention by minocycline. Glia 63, 1825–1839.

Silva R. M., Ries V., Oo T. F. et al. (2005) CHOP/GADD153 is a mediator of apoptotic death in substantia nigra dopamine neurons in an in vivo neurotoxin model of parkinsonism. J. Neurochem. 95, 974–986.

Sim F. J., Zhao C., Penderis J. and Franklin R. J. (2002) The age-related decrease in CNS remyelination efficiency is attributable to an impairment of both oligodendrocyte progenitor recruitment and differentiation. J. Neurosci. 22, 2451–2459.

Simonishvili S., Jain M. R., Li H., Levison S. W. and Wood T. L. (2013) Identification of Bax-interacting proteins in oligodendrocyte progenitors during glutamate excitotoxicity and perinatal hypoxia-ischemia. ASN Neuro 5, e00131.

Slowik A., Schmidt T., Beyer C., Amor S., Clarner T. and Kipp M. (2015) The sphingosine 1-phosphate receptor agonist FTY720 is neuroprotective after cuprizone-induced CNS demyelination. Br. J. Pharmacol. 172, 80–92.

Song B., Scheuner D., Ron D., Pennathur S. and Kaufman R. J. (2008) Chop deletion reduces oxidative stress, improves beta cell function, and promotes cell survival in multiple mouse models of diabetes. J. Clin. Investig. 118, 3378–3389.

Southwood C. M., Garbern J., Jiang W. and Gow A. (2002) The unfolded protein response modulates disease severity in Pelizaeus-Merzbacher disease. Neuron 36, 585–596.

Starkov A. A., Fiskum G., Chinopoulos C., Lorenzo B. J., Browne S. E., Patel M. S. and Beal M. F. (2004) Mitochondrial alpha-ketoglutarate dehydrogenase complex generates reactive oxygen species. J. Neurosci. 24, 7779–7788.

Thorp E., Li G., Seimon T. A., Kuriakose G., Ron D. and Tabas I. (2009) Reduced apoptosis and plaque necrosis in advanced atherosclerotic lesions of Apoe-/- and Ldlr-/- mice lacking CHOP. Cell Metab. 9, 474–481.

Trapp B. D. and Stys P. K. (2009) Virtual hypoxia and chronic necrosis of demyelinated axons in multiple sclerosis. Lancet Neurol. 8, 280–291.

Uranova N., Orlovskaya D., Vikhreva O., Zimina I., Kolomeets N., Vostrikov V. and Rachmanova V. (2001) Electron microscopy of oligodendroglia in severe mental illness. Brain Res. Bull. 55, 597–610.

van der Vlies D., Makkinje M., Jansens A., Braakman I., Verkleij A. J., Wirtz K. W. and Post J. A. (2003) Oxidation of ER resident proteins upon oxidative stress: effects of altering cellular redox/antioxidant status and implications for protein maturation. Antioxid. Redox Signal. 5, 381–387.

Vostrikov V., Orlovskaya D. and Uranova N. (2008) Deficit of pericapillary oligodendrocytes in the prefrontal cortex in schizophrenia. World J. Biol. Psychiatry 9, 34–42.

Wakabayashi N., Itoh K., Wakabayashi J. et al. (2003) Keap1-null mutation leads to postnatal lethality due to constitutive Nrf2 activation. Nat. Genet. 35, 238–245.

Witte M. E., Mahad D. J., Lassmann H. and van Horssen J. (2014) Mitochondrial dysfunction contributes to neurodegeneration in multiple sclerosis. Trends Mol. Med. 20, 179–187.

Zinszner H., Kuroda M., Wang X., Batchvarova N., Lightfoot R. T., Remotti H., Stevens J. L. and Ron D. (1998) CHOP is implicated in programmed cell death in response to impaired function of the endoplasmic reticulum. Genes Dev. 12, 982–995.

8. Veröffentlichung II

Miriam Scheld, Athanassios Fragoulis, Stella Nyamoya, Adib Zendedel, Bernd Denecke, Barbara Krauspe, Nico Teske, Markus Kipp, Cordian Beyer and Tim Clarner, Mitochondrial Impairment in Oligodendroglial Cells Induces Cytokine Expression and Signaling, Journal of Molecular Neuroscience, doi: 10.1007/s12031-018-1236-6, (2018).

Journal of Molecular Neuroscience (2019) 67:265–275
https://doi.org/10.1007/s12031-018-1236-6

Mitochondrial Impairment in Oligodendroglial Cells Induces Cytokine Expression and Signaling

Miriam Scheld[1] &Athanassios Fragoulis[2] &Stella Nyamoya[1,3] &Adib Zendedel[1] &Bernd Denecke[4] &Barbara Krauspe[5] &Nico Teske[3] &Markus Kipp[6] &Cordian Beyer[1] &Tim Clarner[1]

Received: 25 July 2018 / Accepted: 28 November 2018 / Published online: 13 December 2018

Abstract

Widespread inflammatory lesions within the central nervous system grey and white matter are major hallmarks of multiple sclerosis. The development of full-blown demyelinating multiple sclerosis lesions might be preceded by preactive lesions which are characterized by focal microglia activation in close spatial relation to apoptotic oligodendrocytes. In this study, we investigated the expression of signaling molecules of oligodendrocytes that might be involved in initial microglia activation during preactive lesion formation. Sodium azide was used to trigger mitochondrial impairment and cellular stress in oligodendroglial cells in vitro. Among various chemokines and cytokines, IL6 was identified as a possible oligodendroglial cell-derived signaling molecule in response to cellular stress. Relevance of this finding for lesion development was further explored in the cuprizone model by applying short-term cuprizone feeding (2–4 days) on male C57BL/6 mice and subsequent analysis of gene expression, in situ hybridization and histology. Additionally, we analyzed the possible signaling of stressed oligodendroglial cells in vitro as well as in the cuprizone mouse model. In vitro, conditioned medium of stressed oligodendroglial cells triggered the activation of microglia cells. In cuprizone-fed animals, IL6 expression in oligodendrocytes was found in close vicinity of activated microglia cells. Taken together, our data support the view that stressed oligodendrocytes have the potential to activate microglia cells through a specific cocktail of chemokines and cytokines among IL6. Further studies will have to identify the temporal activation pattern of these signaling molecules, their cellular sources, and impact on neuroinflammation.

Keywords Oligodendrocytes · Cytokines · Multiple sclerosis · Preactive lesions · IL6 · Microglia

Electronic supplementary material The online version of this article (https://doi.org/10.1007/s12031-018-1236-6) contains supplementary material, which is available to authorized users.

* Miriam Scheld
mscheld@ukaachen.de

[1] Institute of Neuroanatomy, Faculty of Medicine, RWTH Aachen University, Wendlingweg 2, 52074 Aachen, Germany

[2] Department of Anatomy and Cell Biology, Faculty of Medicine, RWTH Aachen University, 52074 Aachen, Germany

[3] Department of Neuroanatomy, Faculty of Medicine, Ludwig-Maximilians-University of Munich, 80336 Munich, Germany

[4] IZKF Genomics Facility, Interdisciplinary Center for Clinical Research, RWTH Aachen University, 52074 Aachen, Germany

[5] Clinic for Gynaecology and Obstetrics, Faculty of Medicine, RWTH Aachen University, 52074 Aachen, Germany

[6] Institute of Anatomy, Faculty of Medicine, University of Rostock, 18057 Rostock, Germany

Introduction

Stressed oligodendrocytes in close proximity to foamy macrophages and clustered microglia expressing HLA-DR are found widespread within the normal appearing white matter of multiple sclerosis (MS) patients (De Groot et al. 2001; Zeis et al. 2009). These preactive lesions are thought to precede the development of full-blown demyelinating MS lesions (De Groot et al. 2001; Wuerfel et al. 2004; van der Valk and Amor 2009). Therefore, it seems reasonable to assume that the initial microglia activation and clustering as observed in preactive lesions might be triggered by oligodendrocyte-derived signaling molecules. It has been shown that oligodendrocytes are able to secrete a variety of signaling molecules such as chemokines and cytokines and other regulatory proteins which are known to be involved in the regulation of immunological processes (Cannella and Raine 2004; Balabanov et al. 2007; Kummer et al. 2007; Okamura et al. 2007; Tzartos et al. 2008; Merabova et al. 2012; Ramesh et al.

2012; Moyon et al. 2015). For example, IFNγ-treated primary rat oligodendrocytes significantly induced the expression of the chemokines CXCL10, CCL2, CCL3, and CCL5 (Balabanov et al. 2007). Furthermore, the cytokines IL6 and IL8 and the chemokine CCL2 were significantly induced in the human oligodendrocyte cell line MO3.13 when confronted with Borrelia burgdorferi. Exposure to the same bacteria caused the induction of IL8 and CCL2 in a dose-dependent manner in primary human oligodendrocytes (Ramesh et al. 2012).

So far, it is not completely understood which processes trigger oligodendrocyte stress and subsequent expression of signaling molecules. One factor leading to oligodendrocyte stress, impaired mitochondrial functions, and increased levels of reactive oxygen species (Wang et al. 2013) might be the accumulation of mutations within the mitochondrial genome. It is known that the mtDNA is prone to mutations with a mutation rate that is about tenfold higher than chromosomal DNA (Linnane et al. 1989). In comparison to other cell populations, oligodendrocytes have a reduced capacity to repair their mtDNA, possibly due to particularities in the expression of factors involved in DNA repairing mechanisms (Hollensworth et al. 2000). With respect to demyelination and oligodendrocyte pathology, both mutations in mitochondrial genes as well as oxidative stress play a role in lesion formation and disease progression in MS and MS-related animal models (Mahad et al. 2008; Mao and Reddy 2010; Su et al. 2013; Draheim et al. 2016).

As the sentinels and injury sensors of the central nervous system (CNS), microglia can be activated by many kinds of mechanical injury and pathological disturbances within the CNS (Perry et al. 1993; Gehrmann et al. 1995). In MS, the magnitude of myelin loss during demyelinating events positively correlates with the number of activated microglia cells (Clarner et al. 2012). Furthermore, microgliosis can be induced by leukocyte infiltration into the CNS (Scheld et al. 2016; Ruther et al. 2017). However, the listed factors are rather unlikely to contribute to the activation of microglia cells during the formation of preactive lesions, since the affected brain regions lack any signs of demyelination, leukocyte infiltration, astrogliosis or inciting agents such as viral or bacterial antigens (Gay et al. 1997; De Groot et al. 2001; Barnett and Prineas 2004; Marik et al. 2007; van der Valk and Amor 2009). A growing body of evidence suggests that stressed oligodendrocytes might be active contributors to MS lesion formation by initiating microglia reactivity. Barnett and Prineas have reported areas with an extensive oligodendrocyte apoptosis and consultant microgliosis in the absence of infiltrating immune cells in the normal appearing white matter of MS patients, thus indicating that oligodendrocyte loss precedes inflammatory demyelination (Barnett and Prineas 2004).

In this study, we use the oligodendroglial cell line OLN93 to screen for oligodendrocyte-derived chemokines and cytokines that are potentially able to activate microglia cells. Subsequent culture experiments with the microglia cell line BV2 show that IL6, which is robustly expressed by stressed oligodendroglial cells, is a constituent of a cocktail of secreted proteins, which are responsible for microglia activation. Finally, IL6 expression was explored in the cuprizone model, which recapitulates distinct but important aspects of early MS lesion formation.

Materials and Methods

Cell Culture

Cells of the oligodendroglial lineage cell line OLN93 were received from Dr. Richter-Landsberg (RRID: CVCL_5850; Oldenburg, Germany) and chosen as a model system because of strong similarities to primary oligodendrocytes regarding morphology and gene expression (Richter-Landsberg and Heinrich 1996). BV2 cell line was cultured according to Dr. E. Blasi (RRID: CVCL_0182; Modena, Italy) and chosen as a model system because of its suitability to study molecular mechanisms that control induction and expression of biological activities in microglia (Blasi et al. 1990). Cell lines were not authenticated prior to experiments. None of the cell lines used in these experiments is listed as a commonly misidentified cell line by the International Cell Line Authentication Committee. OLN93 oligodendroglial cell line and BV2 microglial cell lines were maintained in Dulbecco's Modified Eagle Medium supplemented with 5% (OLN93) and 10% (BV2) heat-inactivated fetal bovine serum, penicillin G (10,000 units/mL), and streptomycin (10,000 µg/mL). For experiments, cells were seeded into 6-well dishes, 10 cm culture dishes or 75 cm^2 flasks at densities of 3×10^5, 5×10^6, and 2.3×10^6 cells per well, respectively. Before treatment, cells were cultivated for 24 h in starving medium (OLN93: SATO with 1% penicillin G/streptomycin; BV2: DMEM supplemented with 0.5% fetal calf serum and 0.5% penicillin G/streptomycin). Cells were cultivated in a humidified atmosphere of 5% CO_2 at 37 °C.

Oligodendroglial Cell-Conditioned Medium (OCM)

OLN93 cells were treated with 10 mM sodium azide (SA, Sigma Aldrich) or vehicle (UltraPure Distilled Water; Thermo Fisher Scientific) for 24 h. After washing twice with 1× phosphate buffered saline (PBS), cells were incubated with starving medium for a 24 h secretion period. The medium of each treatment group was pooled, centrifuged, and filtered through a 20 µm cell strainer. BV2 microglia were incubated with OCM from SA-treated cells (OCM-SA) for 6 h. Oligodendroglial starving medium and OCM from vehicle groups (OCM-vehicle) served as control. OCM was

additionally used for ELISA analysis (see supplementary figure A for experimental overview).

Cell Viability and Metabolic Activity Assay

To investigate the toxic effects of the applied SA concentrations, CytoTox 96® Non-Radioactive Cytotoxicity Assay and CellTiter-Blue® Cell Viability Assay (Promega G1780, G8081) were performed according to the manufacturer's instructions. Briefly, cells were seeded into an opaque-walled 96 tissue culture plate and treated with SA and vehicle for 24 h. Treatment of cells with a lysis solution served as a negative control as all cells are dead; medium without cells served as blank. Cells were incubated with CellTiter-Blue reagent until a change of color was observed; fluorescence was measured at 560/590 nm with the Tecan infinite M200 plate reader and processed with i-control 1.10 software. Medium of cells was incubated for 30 min with CytoTox96 reagent and the reaction was stopped with stop solution. Absorbance was measured at 490 nm with Tecan i-control software. Data are given in % of control fluorescence and absorbance values, respectively. No blinding was performed for the evaluation of these data. Experiments were performed with eight biological and two technical replicates.

Enzyme-linked Immunosorbent Assay

IL6 ELISA was conducted using cell culture supernatants of vehicle and SA-treated OLN93 cells (OCM) according to the manufacturer's protocol (Quantikine ELISA, R&D Systems). Color development of substrate solution (stabilized hydrogen peroxide and stabilized chromogen (tetramethylbenzidine)) was monitored with a Tecan infinite M200 plate reader at 450 nm with a wavelength correction at 540 nm and processed with i-control 1.10 software. IL6 protein levels are displayed as absolute values in pg/ml. Experiments were performed with two biological and two technical replicates.

Animals and Cuprizone Intoxication

C57BL/6J male mice (19 ± 2 g) were obtained from Janvier and housed under standard laboratory conditions in the animal facility of the Uniklinik Aachen according to the Federation of European Laboratory Animal Science Association's recommendations. Mice were maintained with food and water ad libitum in a 12 h light/dark cycle at controlled temperature and humidity (23 ± 2 °C, 55 % ± 10 % humidity). Experimental procedures, i.e., cuprizone feeding, were approved by the Review Board for the Care of Animal Subjects of the district government (Nordrhein-Westfalen, Germany). At noon, mice received a diet containing 0.25 % cuprizone (bis-cyclohexanone-oxaldihydrazone; Sigma Aldrich; choice of concentration via established protocols) for up to 2 days mixed into a ground standard rodent chow. The control group was fed with standard rodent chow. Animals were allocated to groups applying the following procedure. Animals were distributed across cages (three animals per cage; cage area 430 cm^2) and each group consisted of mice with comparable weight. We used cards numbered from 1 to 2 for the respective experimental group (1 = control, 2 = 2 days cuprizone). The number on the card randomly assigned the cages to the respective group. Re-evaluation of cDNA samples of 1–4 days cuprizone-treated mice were performed using previously published work from our research group (Krauspe et al. 2015). Size of groups for each experiment is given in the appropriate figure legends and an experimental overview is shown in supplementary figure B.

Tissue Preparation

Mice were anaesthetized with ketamine/xylazine (100 mg/kg and 10 mg/kg; i.p. with 100 µl/10 g body weight) and transcardially perfused with either PBS or 3.7% formalin in PBS. Brains were removed to isolate RNA of the corpus callosum (CC) for gene expression analysis or whole brains were post-fixed in 3.7% formalin and subsequently embedded into paraffin for immunohistological analysis following established protocols (Clarner et al. 2015).

Immunohistological Staining and Fluorescence Labeling

For fluorescence and immunohistological analysis, 5 µm thick brain slides were cut with a microtome. Rabbit anti-IL6 (Abcam ab7737), mouse anti-OLIG2 (Millipore MABN50), donkey-anti-rabbit 488, and donkey-anti-mouse 594 were used for fluorescence labeling (Life Technologies A21206, A21203). Signal specificity was validated by incubating slices with the respective secondary antibody without pre-incubation with the first antibody (see supplementary figure C). Furthermore, cross reactivity of secondary antibodies with each other or the false primary antibody was additionally excluded (data not shown). For chromogen double labeling, anti-GFAP (Santa Cruz sc-6170), anti-IBA-1 (Millipore MABN92), and anti-APC (Millipore OP80) antibodies were visualized with a horseradish peroxidase enzyme (Vector Labs) and DAB substrate (Dako); anti-IL6 (Abcam ab6672) was visualized with an alkaline phosphatase (Zytomed Systems) and an AP Blue substrate that emits at 680 nm (Vector Laboratories).

In Situ Hybridization

Commercial fluorescence in situ hybridization kits (QuantiGene View RNA in situ hybridization tissue assay; Affymetrix-Panomics) were used for double labeling of formalin-fixed, paraffin-embedded tissue, following the manufacturer's recommendations. Protease digestion time was adjusted

to 20 min. Probes directed against Olig2 and Il6 were purchased from Affymetrix (Affymetrix-Panomics). Confocal images were captured using the LSM710 laser-scanning microscope station (Carl Zeiss).

Chemokine and Cytokine Array

RNA isolation was performed with RNeasy Micro Kit (Qiagen 74004). Cells were directly lysed with RLT buffer and homogenized with Precellys homogenizer. Further isolation procedures such as washing and DNA digestion were conducted in MinElute spin columns. RNA concentration was measured with NanoDrop 1000 spectrometer. Five hundred nanograms of RNA were reverse-transcribed with RT^2 First Strand Kit (Qiagen 330404). Genomic DNA was eliminated and RNA reverse-transcribed according to the manufacturer's instructions. Cytokine & Chemokine RT^2 Profiler PCR Array (Qiagen PARN-150ZD) was performed with RT^2 SYBR Green Mastermix and processed with Bio-Rad CFX connect cycler. PCR cycling program was composed of one 10 min 95 °C hot start cycle and 40 cycles of 95 °C 15 s and 60 °C 1 min to perform fluorescence data collection. Results were analyzed using the Data analysis center from Qiagen (https://www.qiagen.com/de/shop/genes-and-pathways/data-analysis-center-overview-page/). β-Actin, β-2 microglobulin, hypoxanthine phosphoribosyltransferase 1, lactate dehydrogenase A, and ribosomal protein large P1 served as reference genes. Furthermore, the array contained one genomic DNA control, three replicate reverse-transcription controls to test reverse-transcription efficiency, and three replicate positive PCR controls to test PCR efficiency. Experiments were performed with one biological and one technical replicate.

Gene Expression Analysis

RNA for array validation and microglia gene expression analysis was isolated by using peqGold TriFast (Peqlab) and reverse-transcribed in a 20 µL reaction volume using a reverse-transcription kit (Thermo Fisher Scientific 28025-021). cDNA levels were then analyzed by qPCR using SensiMix SYBR® & Fluorescein Kit (Bioline QT615-05) and Bio-Rad CFX connect cycler. The expression levels were calculated relative to the reference genes coding for glyceraldehyde 3-phosphate dehydrogenase or cyclophilin A using the ΔΔCt method. Primer sequences are given in Table 1. No blinding was performed for the evaluation of these data. Experiments were performed with at least six biological and two technical replicates if not stated otherwise. Furthermore, a gene array (Affymetrix) from the corpus callosum (CC) of control animals and animals that were fed cuprizone for 2 days was re-evaluated with respect to those genes identified in the OLN93 gene expression study (Krauspe et al. 2015).

Statistical Analysis

Statistical analysis was performed using JMP10 and GraphPad Prism 5. Data are presented as arithmetic means ± SEM. To test for equal variances, Bartlett test was performed. Data transformations via Boxcox for homoscedasticity are indicated if necessary. Shapiro-Wilk test was used to test for normal distribution. Parametric data were analyzed with one-way ANOVA followed by Tukey's post hoc test for multiple comparisons or with Student's t test. Non-parametric data were analyzed with Kruskal-Wallis test followed by the Dunn's multiple comparison or Mann-Whitney U test. $p < 0.05$ was considered statistically significant. The following symbols were used to indicate the level of significance: *$p < 0.05$, **$p < 0.005$, ***$p < 0.001$; ns indicates not significant. No outliers were excluded from the analyses. No sample size calculation was performed.

Results

Sodium Azide Induces Stress in Oligodendroglial Cells

SA is a potent inhibitor of the mitochondrial respiratory chain and inhibits the mitochondrial complex IV which is responsible for the transfer of cytochrome c to an oxygen molecule (Bennett et al. 1996; Teske et al. 2018). To induce a breakdown of the mitochondrial inner transmembrane potential (i.e., sub-lethal mitochondrial stress reaction), the oligodendroglial cell line OLN93 was stimulated with 10 mM sodium azide (SA) for 24 h as previously described by Teske et al. (2018). Afterwards, cells were kept in culture for additional 24 h to produce OCM (oligodendroglial cell-conditioned medium). To confirm that the used SA concentration was not inducing immediate cell death, lactate dehydrogenase (LDH) cytotoxicity assay and cell titer blue (CTB) viability assay were performed after 24 h of SA-treatment. Results are shown in Fig. 1a. LDH levels in the cell culture supernatants were significantly increased after SA treatment compared to vehicle, indicating cell death; LDH levels of lysis control were significantly increased compared to both treatment groups (left histogram in Fig. 1a). SA-induced LDH release was paralleled by a trend towards lower levels of metabolic activity in these cells (right histogram in Fig. 1a); however, this difference was not statistically significant. Additionally, 10 mM SA-treated OLN93 cells did not show major morphological changes or loss of cell numbers at the microscopic level (Fig. 1b). DDIT3 and ATF3 are members of the integrated stress response which is closely connected to oxidative stress (Rutkowski et al. 2006; Puthalakath et al. 2007) and Atf3 (Fujiwara et al. 2014) was measured after the 24 h secretion phase via qPCR to confirm endoplasmic reticulum stress in SA-treated cells on the transcriptional level (Fig. 1c).

Table 1 Forward and reverse primer sequences used for qPCR analysis

Name	Forward sequence 5′-3′	Reverse sequence 5′-3′
Arg1 mouse	CTCCAAGCCAAAGTCCTTAGAG	AGGAGCTGTCATTAGGGACATC
Atf3 rat	ACTGCGTTGTCCCACTCTGT	TCATCTGAGAATGGCCGGGA
Csf1 rat	AGCAAGGAAGCGAACGAAC	ATGTGGCTACAGTGCTCCGA
Cyca rat	GGCAAATGCTGGACCAAACAC	TTAGAGTTGTCCACAGTCGGAGATG
Ddit3 rat	TGTTGAAGATGAGCGGGTGG	GCTTTCAGGTGTGGTGGTGT
Gapdh mouse	TGTGTCCGTCGTGGATCTGA	CCTGCTTCACCACCTTCTTGA
Gdf15 rat	TCAGCTGAGGTTCCTGCTGTTC	GCTCGTCCGGGTTGAGTTG
Il6 mouse	GATACCACTCCCAACAGACCTG	GGTACTCCAGAAGACCAGAGGA
Il6 rat	TCTCTCCGCAAGAGACTTCCA	ATACTGGTCTGTTGTGGGTGG
Lif rat	TTTGCCGTCTGTGCAACAAG	TGGACCACCGCACTAATGAC
Nos2 mouse	ACATCGACCCGTCCACAGTAT	CAGAGGGGTAGGCTTGTCTC
Spp1 rat	CCAGCCAAGGACCAACTACA	TCTCCTCTGAGCTGCCAAAC

Stressed Oligodendroglial Cells Secrete Various Cytokines and Chemokines

In a next step, we aimed to analyze the gene expression of stressed molecules that oligodendroglial cells produce upon SA-induced mitochondrial stress. To get a first hint about the possible identity of such signaling molecules, we performed PCR array that screened for mRNA expression levels of 84 cytokines and chemokines with one sample (n = 1). Out of the 84 investigated genes, 13 were induced by at least twofold when comparing the SA group with the vehicle group. Those 13 genes are displayed in Fig. 2a. IL6 and GDF15 were most robustly induced in stressed oligodendroglial cells compared to cells treated with vehicle. To confirm validity of the path finding gene array, we performed qPCR in independent samples from two additional experiments with each n = 6 for IL6, GDF15, and three randomly assigned genes (Fig. 2b). As indicated in Fig. 2b, IL6 gene expression and GDF15 gene expression were found to be induced > 12-fold in qPCR analysis in SA-treated OLN93 cells. Differences in between the gene expression measured in array analysis versus qPCR are likely due to different evaluation strategies, i.e., different reference genes and subsequent software analysis and the measuring of only one sample in the PCR array. In comparison, genes for SPP1, LIF, and CSF1 were induced 2.5- to 4-fold. In a next step, the relevance of the identified factors in vivo was investigated. Since short-term cuprizone intoxication mimics early lesion formation and induces stress in oligodendroglial cells (Fig. 2g), we re-evaluated gene array data from the CC of 2-day cuprizone-fed and control animals (Krauspe et al. 2015). Results of this evaluation are shown in Fig. 2c. Out of the 13 investigated genes, 7 were significantly induced. Although GDF15 and CCL7 were highest induced in the tissue samples from cuprizone-fed animals, oligodendroglial cells might be responsible—at least in part—for the increased IL6 expression in vivo. In a next step, we investigated whether oligodendroglial cells secrete IL6 on the protein level. Therefore, sandwich ELISA was performed using OCM from SA-treated and vehicle-treated oligodendroglial cells. Results are shown in Fig. 2e and demonstrate a fourfold increase in IL6 levels upon SA-treatment. Our data show that stressed oligodendroglial cells express various signaling molecules that potentially activate microglia cells. To further investigate this hypothesis, the activation state of microglia cells was evaluated in OCM-stimulated BV2 microglia. Morphologically, no differences were found between cells growing in control medium (DMEM 0.5 %) and those cells grown in OCM-SA. Representative pictures after 6 h incubation time are shown in Fig. 2d. Additionally, performed arborization analysis and counting of bipolar cells did not reveal morphological changes in response to OCM-SA (supplementary figure E). Expression levels of typical pro- and anti-inflammatory microglia markers were measured by means of qPCR 6 h after beginning of treatment (see supplementary figure A for experimental overview). Results of these experiments are shown in Fig. 2f. Gene expression of the anti-inflammatory marker arginase 1 was induced when BV2 microglia cells were treated with OCM from SA-treated oligodendroglial cells compared to OCM-vehicle-treated BV2 microglia. One factor that is known to be induced in microglia cells upon pro-inflammatory stimulation is NOS2 (Kempuraj et al. 2016). OCM-SA-treated BV2 microglia displayed an induced expression of NOS2 compared to control. Blocking of IL6 with anti-IL6 antibody only partly counteracted OCM-SA effects (Fig. 2g), and none of the used concentrations of IL6 protein (10, 30, and 50 ng/ml) was sufficient to show BV2 microglia responses with respect to the gene expression of both Nos2 and Arg1, indicating that other secreted molecules contribute to microglia activation in this scenario (supplementary figure F).

Oligodendrocytes are a Source of IL6 In Vivo

To investigate whether oligodendrocytes might be a relevant source of signaling molecules in vivo, we included short-term

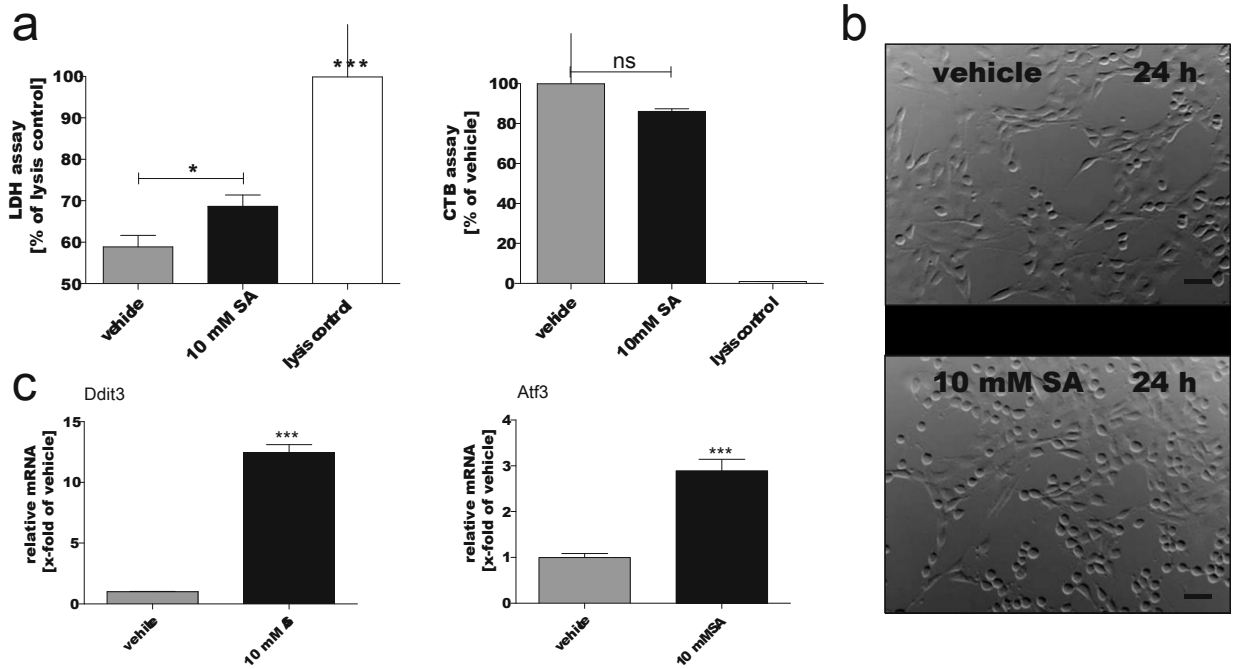

Fig. 1 a The cytotoxicity (left) assay normalized to the lysis control and cell viability (right) assay normalized to the vehicle-treated cells of SA and vehicle-treated OLN93 cells (eight culture wells, one experiment). b Microscopic pictures using the FLoid™ Cell Imaging station (Thermo Fisher Scientific) of vehicle and SA-treated oligodendroglial cells did not reveal obvious signs of cell loss or death (× 20 magnification, scale bar 50 μm). c Gene expression analysis of Ddit3 and Atf3 (BoxCox-Y transformed) in vehicle- and SA-treated oligodendroglial cells indicating metabolic stress (at least six culture wells, five independent experiments). ns, not significant; *p < 0.05; **p < 0.005; ***p < 0.001; vehicle, μOL-1

cuprizone-intoxicated mice (up to 4 days cuprizone) in the study. Since IL6 was highly induced in oligodendroglial cells in vitro, we focused on this molecule in this part of the study. Immunohistochemistry, qPCR, and in situ hybridization were performed on brain slices of cuprizone-intoxicated animals. After 2 days of cuprizone intoxication, IBA-1 immunohistochemistry revealed that microglia display an activated cell morphology in the CC (i.e., less ramified, swollen somata) compared to control mice (Fig. 3a). Similar morphological changes as well as an increase in microglia cell numbers in early cuprizone-induced lesions have been published previously by our group after a 2-day exposure to cuprizone (Clarner et al. 2015; Krauspe et al. 2015). Re-evaluation via qPCR revealed that IL6 gene expression was increased about fivefold in the CC after 2 days of cuprizone intoxication ((Krauspe et al. 2015), Fig. 3b, n ≥ 3). This induction further increased up to 17-fold after 4 days of cuprizone intoxication. In situ hybridization showed an increase of IL6 mRNA signals in the CC of cuprizone-intoxicated animals compared to controls (Fig. 3c, left panel). Double in situ hybridization (Fig. 3c, right panel) and validation by fluorescence double labeling of Olig2 and IL6 proteins (Fig. 3d) as well as double chromogen labeling of APC and IL6 proteins (Fig. 3e) revealed oligodendroglial cells as one source of IL6 at this early time point (see supplementary figure B for experimental overview). Although APC labels astrocytes and neurons in the brain as well, the double-positive cell in Fig. 3e resembles morphologically strongly an oligodendrocyte. Three cuprizone-fed animals were investigated and IL6/Olig2- and IL6/APC-positive cells were found in the CC in all three animals. Since confocal Z-stack analysis was necessary to undoubtedly identify double-positive cells, no quantification of the number of these cells could be performed. Note that oligodendrocytes are not the sole source of IL6 but also other glial cells such as astrocytes express IL6 after 2 days of cuprizone feeding (see supplementary figure D). Tezuka and colleagues also identified astrocytes as a source of IL6 in this model (Tezuka et al. 2013).

Discussion

The contribution of stressed oligodendrocytes to the formation of inflammatory CNS lesions is only incompletely understood. Here, we induced oligodendrocyte stress by using the mitochondrial inhibitor SA in vitro and cuprizone intoxication in vivo. In vitro, this treatment caused a selective increase in the oligodendroglial expression of a variety of immune-modulatory factors such as IL6, GDF15, and a number of chemokines. The expression of IL6 in the in vivo situation was explored by qPCR analysis, ELISA, in situ hybridization,

a

Gene Symbol	Il6	Gdf15	Cxcl3	Cxcl1	Ccl5	Spp1	Cxcl11	Lif	Csf1	Ccl7	Ccl4	Cxcl12	Il18
Fold regulation	40.50	34.99	9.88	4.44	4.41	3.80	3.71	2.73	2.52	2.32	2.23	2.17	2.05

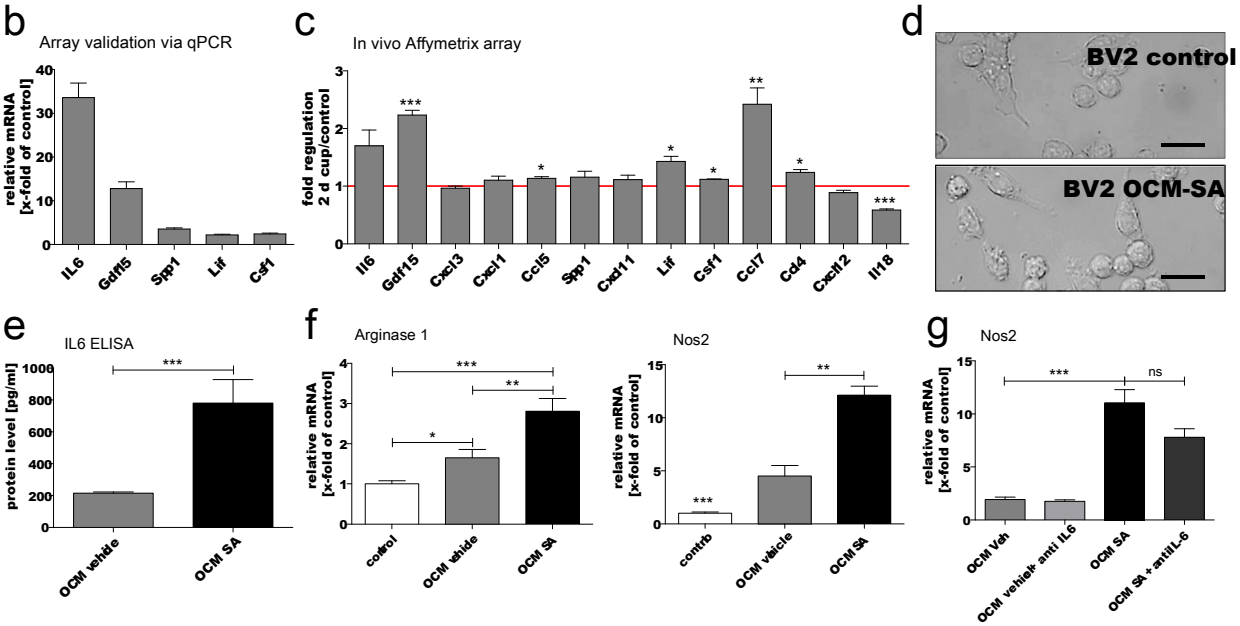

Fig. 2 a The fold difference of all chemokines and cytokines that were induced at least twofold in SA-treated OLN93 cells compared to control in the PCR array. b To validate the PCR array results, the gene expression was analyzed via qPCR on independent samples (at least six culture wells, two independent experiments). In c, the re-evaluation of a gene array from the CC of 2-day cuprizone-intoxicated mice is shown. Data are displayed as fold induction of control. Note that a selective induction of the identified factors in oligodendroglial cells might be obscured due to the fact that this array measured expression in the whole tissue and not exclusively in oligodendrocytes (three animals per group, one experiment, see Krauspe et al. 2015). d Representative pictures after 6 h incubation time of BV2 microglia cells with OCM-SA and DMEM 0.5% (control). e IL6 protein levels increased up to fourfold in stressed oligodendroglial cells versus unstressed oligodendroglial cells (BoxCox-Y transformed, six samples each group, two independent experiments). The gene expression results of pro- and anti-inflammatory markers arginase 1 (BoxCox-Y transformed) and Nos2 of OCM-stimulated microglia cells (at least five culture wells, four independent experiments). g Induction of Nos2 expression by OCM was partly (not significant) counteracted by anti-IL6 antibody in the media. ns, not significant; *p < 0.05; **p < 0.005; ***p < 0.001; vehicle, 2% FCS; scale bars, 30 µm

and immunohistological staining of tissue from short-term cuprizone-intoxicated mice. Fluorescence double-labeling and in situ hybridization of OLIG2/APC and IL6 identified oligodendrocytes as a possible source of this molecule in vivo (Ramesh et al. 2012). These results indicate that our in vitro data obtained from SA-treated oligodendroglial cells might be relevant for the in vivo situation. It has to be mentioned at this point, that oligodendrocytes are not the sole source of these molecules in vivo. With respect to IL6, astrocytes and microglia have been shown to be additional sources in cuprizone intoxication. We would like to point out that due to the high number of possibly involved molecules and the highly complex interplay of different glia cells in the formation of early inflammatory lesions, knock-out mice deficient for single molecules would be of limited use to further investigate the role of oligodendrocytes in this scenario.

Regarding the role of IL6 in CNS inflammation and regeneration in general, it has been shown that on one hand it is neuroprotective via accelerating nerve regeneration following trauma or spinal cord injury (Hirota et al. 1996; Yang et al. 2012) and protects mice from demyelination in the cuprizone model by inducing a specific activation state in microglia (Petkovic et al. 2017). On the other hand, IL6 supports chronic inflammatory processes in disorders such as Alzheimer's disease (Swardfager et al. 2010). In active demyelinating MS lesions, IL6 expression by astrocytes and macrophages is relevant for the preservation of oligodendrocytes (Schonrock et al. 2000). IL6 signaling and mitochondrial functions are closely linked, since IL6 protects cells against a loss of mitochondrial complex IV after bacterial infection in mice (Maiti et al. 2015). In the liver, IL6 is necessary for the repair of mitochondrial mutations caused by ethanol intoxication (Zhang et al. 2010).

The physiological IL6 concentration in blood plasma samples from healthy humans is about 1–1.5 pg/ml, whereas the concentration in inflammatory conditions is highly increased and might reach up to 1,000 pg/ml in sever inflammation (Damas et al. 1992; Seino et al. 1994; Ridker et al. 2000). This is comparable to the concentrations we measured in the medium of stressed oligodendroglial cells (app. 800 pg/ml). Regarding the IL6 concentrations within the brain, both in healthy and inflamed tissue, only little is known. Therefore, further studies will have to show the local IL6 concentrations and precise source within brain tissue in distinct pathologies. With respect to microglia cells, it has been shown that a concentration of 100 ng/ml does activate Nos2 mRNA expression in BV2 microglia (Matsumoto et al. 2018). Furthermore, IL6 (50 ng/ml) increases the mitochondrial Ca^{2+} levels in a STAT3-dependent manner in $CD4^+$ T cells (Yang et al. 2015). By using Luciferin-expressing mice, we recently demonstrated that cuprizone intoxication causes an early induction of Nrf2-ARE signaling within the brain (Draheim et al. 2016). Since Nrf2 has been shown to regulate IL6 expression (Wruck et al. 2011), the increase in oxidative stress and subsequent Nrf2-activation might be a possible mechanism by which IL6 expression is initially triggered in oligodendrocytes in this model. Further studies including Nrf2-deficient mice will have to show the link between oxidative stress and Nrf2 activity on one hand and the expression of IL6 in oligodendrocytes on the other hand. Given this data, we consider this early IL6 expression by oligodendrocytes during preactive lesion formation as a potential first B cell „for help" by metabolically dysfunctional or oxidatively challenged oligodendrocytes.

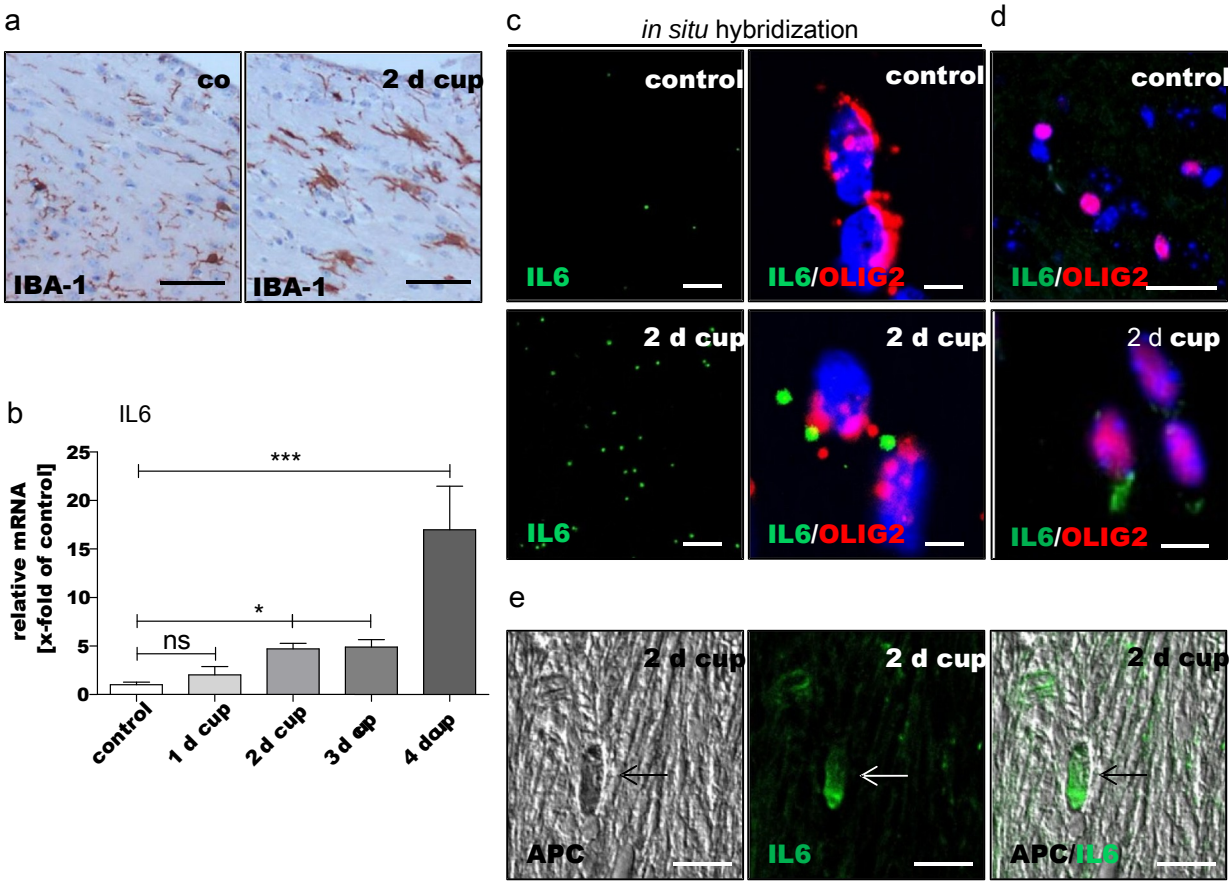

Fig. 3 a IBA-1 $^+$ microglia cells display an activated morphology upon short-term cuprizone intoxication compared to control mice (scale bars 50 µm). b IL6 gene expression was increased in the CC after 2, 3, and 4 days of cuprizone intoxication compared to untreated animals (re-evaluation of cDNA of short-term cuprizone-fed mice, BoxCox-Y transformed). c At 2 days of 0.25% cuprizone intoxication, the signal for IL6 mRNA was increased compared to the control. In situ hybridization of OLIG2 and IL6 identified oligodendrocytes as a source of IL6 production after short-term cuprizone intoxication (scale bars for IL6 20 µm; for IL6/OLIG2 5 µm), which was further validated via d fluorescence double-labeling of OLIG2 and IL6 (scale bars for control 25 µm; for 2-day cup 10 µm). e Double labeling of IL6 and APC (scale bars 10 µm) (three animals per group, one experiment for figure a–e). ns, not significant; *p < 0.05; **p < 0.005; ***p < 0.001

Another member of the IL6 cytokine family that was induced upon SA-stimulation in this study is LIF, which signals through the JAK/STAT pathway as well. It is required for the induction of inflammatory responses of microglia and astrocytes to brain damage (Holmberg and Patterson 2006). Furthermore, it has been shown that LIF plays a role in the initial infiltration of inflammatory cells into the CNS and in the neuronal response to brain injury (Sugiura et al. 2000). Another highly induced molecule in our study was GDF15, also known as macrophage inhibitory cytokine-1. Bonaterra et al. showed that GDF15 is functionally linked to IL6 signaling since it regulates inflammatory IL6-dependent processes in vascular injury (Bonaterra et al. 2012). A study on the tumorigenesis of prostate carcinoma indicated that the expression of GDF15 is upregulated by IL6 (Tsui et al. 2012). Despite these links to IL6 signaling, GDF15 plays a major role in regulating inflammatory pathways in injured tissues and is involved in pathological processes such as cancer, cardiovascular disorders, ischemia, and atherosclerosis (Schlittenhardt et al. 2005; Kempf et al. 2006; Jiang et al. 2016).

A number of chemokines were induced in SA-treated OLN93 cells that are known to be involved in microglia activation, including CXCL1 and CCL5 (Škuljec et al. 2011). The cytokine-like glycoprotein SPP1, also known as osteopontin, was induced about fourfold in stressed oligodendroglial cells. Osteopontin has been implicated in the pathogenesis of several autoimmune diseases such as rheumatoid arthritis, autoimmune hepatitis, and MS (Chabas et al. 2001; Yumoto et al. 2002; Mochida et al. 2004). Furthermore, osteopontin activity is found in MS lesions (Chen et al. 2009). It has been shown that the treatment of mixed cortical cultures with osteopontin leads to a stimulation of myelin basic protein expression and the formation of myelin sheaths indicating a putative role in remyelination and recovery (Selvaraju et al. 2004). CSF1, a macrophage colony-stimulating factor, was induced 2.5-fold in SA-stressed oligodendroglial cells and is involved in the proliferation, differentiation, and chemotactic activity of monocytes and macrophages. Interestingly, the survival of adult murine microglia cells seems to be fully dependent upon CSF1 receptor signaling, since all microglia cells can be eliminated from the CNS through CSF1R inhibitor administration (Elmore et al. 2014).

All of the abovementioned signaling molecules might account—either alone or in combination—for the effects, observed in OCM-treated microglia cells. Our data indicate that not a sole oligodendroglial cell-derived molecule but rather a combination of different factors account for the activation of microglia cells.

In summary, our data supports the view that stressed oligodendrocytes have the potential to activate microglia cells through a specific cocktail of chemokines and cytokines such as IL6. Further studies will have to identify the temporal activation pattern of these signaling molecules, their cellular sources and their impact on neuroinflammation.

Acknowledgements The excellent support by Helga Helten, Petra Ibold and Uta Zahn is appreciated. We thank Prof. Dr. Reinhard Windoffer and Dr. Volker Buck for their assistance with confocal microscopy and PD Dr. Claudia Krusche for technical support.

Funding Information Grantsponsor: This study was funded by the START program of the medical faculty of the RWTH Aachen University (M.S.).

Compliance with ethical standards

Conflict of Interest The authors declare that they have no conflict of interest.

References

Bhalabanov R, Strand K, Goswami R, McMahon E, Begolka W, Miller SD, Popko B (2007) Interferon-gamma-oligodendrocyte interactions in the regulation of experimental autoimmune encephalomyelitis. J Neurosci 27(8):2013–2024

Barnett MH, Prineas JW (2004) Relapsing and remitting multiple sclerosis: pathology of the newly forming lesion. Ann Neurol 55(4):458–468

Bennett MC, Mlady GW, Kwon YH, Rose GM (1996) Chronic in vivo sodium azide infusion induces selective and stable inhibition of cytochrome c oxidase. J Neurochem 66(6):2606–2611

Blasi E, Barluzzi R, Bocchini V, Mazzolla R, Bistoni F (1990) Immortalization of murine microglial cells by a v-raf/v-myc carrying retrovirus. J Neuroimmunol 27(2-3):229–237

Bonaterra GA, Zugel S, Thogersen J, Walter SA, Haberkorn U, Strelau J, Kinscherf R (2012) Growth differentiation factor-15 deficiency inhibits atherosclerosis progression by regulating interleukin-6-dependent inflammatory response to vascular injury. J Am Heart Assoc 1(6):e002550

Cannella B, Raine CS (2004) Multiple sclerosis: cytokine receptors on oligodendrocytes predict innate regulation. Ann Neurol 55(1):46–57

Chabas D, Baranzini SE, Mitchell D, Bernard CC, Rittling SR, Denhardt DT, Sobel RA, Lock C, Karpuj M, Pedotti R, Heller R, Oksenberg JR, Steinman L (2001) The influence of the proinflammatory cytokine, osteopontin, on autoimmune demyelinating disease. Science 294(5547):1731–1735

Chen M, Chen G, Nie H, Zhang X, Niu X, Zang YC, Skinner SM, Zhang JZ, Killian JM, Hong J (2009) Regulatory effects of IFN-beta on production of osteopontin and IL-17 by CD4+ T Cells in MS. Eur J Immunol 39(9):2525–2536

Clarner T, Diederichs F, Berger K, Denecke B, Gan L, van der Valk P, Beyer C, Amor S, Kipp M (2012) Myelin debris regulates inflammatory responses in an experimental demyelination animal model and multiple sclerosis lesions. Glia 60(10):1468–1480

Clarner T, Janssen K, Nellessen L, Stangel M, Skripuletz T, Krauspe B, Hess FM, Denecke B, Beutner C, Linnartz-Gerlach B, Neumann H, Vallieres L, Amor S, Ohl K, Tenbrock K, Beyer C, Kipp M (2015)

CXCL10 triggers early microglial activation in the cuprizone model. J Immunol 194(7):3400–3413
Damas P, Ledoux D, Nys M, Vrindts Y, De Groote D, Franchimont P, Lamy M (1992) Cytokine serum level during severe sepsis in human IL-6 as a marker of severity. Ann Surg 215(4):356–362
De Groot CJ, Bergers E, Kamphorst W, Ravid R, Polman CH, Barkhof F, van der Valk P (2001) Post-mortem MRI-guided sampling of multiple sclerosis brain lesions: increased yield of active demyelinating and (p)reactive lesions. Brain 124(Pt 8):1635–1645
Draheim T, Liessem A, Scheld M, Wilms F, Weissflog M, Denecke B, Kensler TW, Zendedel A, Beyer C, Kipp M, Wruck CJ, Fragoulis A, Clarner T (2016) Activation of the astrocytic Nrf2/ARE system ameliorates the formation of demyelinating lesions in a multiple sclerosis animal model. Glia 64(12):2219–2230
Edagawa M, Kawauchi J, Hirata M, Goshima H, Inoue M, Okamoto T, Murakami A, Maehara Y, Kitajima S (2014) Role of activating transcription factor 3 (ATF3) in endoplasmic reticulum (ER) stress-induced sensitization of p53-deficient human colon cancer cells to tumor necrosis factor (TNF)-related apoptosis-inducing ligand (TRAIL)-mediated apoptosis through up-regulation of death receptor 5 (DR5) by zerumbone and celecoxib. J Biol Chem 289(31): 21544–21561
Elmore MR, Najafi AR, Koike MA, Dagher NN, Spangenberg EE, Rice RA, Kitazawa M, Matusow B, Nguyen H, West BL, Green KN (2014) Colony-stimulating factor 1 receptor signaling is necessary for microglia viability, unmasking a microglia progenitor cell in the adult brain. Neuron 82(2):380–397
Gay FW, Drye TJ, Dick GW, Esiri MM (1997) The application of multifactorial cluster analysis in the staging of plaques in early multiple sclerosis. Identification and characterization of the primary demyelinating lesion. Brain 120(Pt 8):1461–1483
Gehrmann J, Matsumoto Y, Kreutzberg GW (1995) Microglia: intrinsic immuneffector cell of the brain. Brain Res Brain Res Rev 20(3): 269–287
Hirota H, Kiyama H, Kishimoto T, Taga T (1996) Accelerated nerve regeneration in mice by upregulated expression of interleukin (IL) 6 and IL-6 receptor after trauma. J Exp Med 183(6):2627–2634
Hollensworth SB, Shen C, Sim JE, Spitz DR, Wilson GL, LeDoux SP (2000) Glial cell type-specific responses to menadione-induced oxidative stress. Free Radic Biol Med 28(8):1161–1174
Holmberg KH, Patterson PH (2006) Leukemia inhibitory factor is a key regulator of astrocytic, microglial and neuronal responses in a low-dose pilocarpine injury model. Brain Res 1075(1):26–35
Jiang J, Wen W, Sachdev PS (2016) Macrophage inhibitory cytokine-1/growth differentiation factor 15 as a marker of cognitive ageing and dementia. Curr Opin Psychiatry 29(2):181–186
Kempf T, Eden M, Strelau J, Naguib M, Willenbockel C, Tongers J, Heineke J, Kotlarz D, Xu J, Molkentin JD, Niessen HW, Drexler H, Wollert KC (2006) The transforming growth factor-beta superfamily member growth-differentiation factor-15 protects the heart from ischemia/reperfusion injury. Circ Res 98(3):351–360
Kempuraj D, Thangavel R, Natteru PA, Selvakumar GP, Saeed D, Zahoor H, Zaheer S, Iyer SS, Zaheer A (2016) Neuroinflammation induces neurodegeneration. J Neurol Neurosurg Spine 1(1)
Krauspe BM, Dreher W, Beyer C, Baumgartner W, Denecke B, Janssen K, Langhans CD, Clarner T, Kipp M (2015) Short-term cuprizone feeding verifies N-acetylaspartate quantification as a marker of neurodegeneration. J Mol Neurosci 55(3):733–748
Kummer JA, Broekhuizen R, Everett H, Agostini L, Kuijk L, Martinon F, van Bruggen R, Tschopp J (2007) Inflammasome components NALP 1 and 3 show distinct but separate expression profiles in human tissues suggesting a site-specific role in the inflammatory response. J Histochem Cytochem 55(5):443–452
Linnane AW, Marzuki S, Ozawa T, Tanaka M (1989) Mitochondrial DNA mutations as an important contributor to ageing and degenerative diseases. Lancet 1(8639):642–645
Mahad D, Lassmann H, Turnbull D (2008) Review: mitochondria and disease progression in multiple sclerosis. Neuropathol Appl Neurobiol 34(6):577–589
Mahi AK, Sharba S, Navabi N, Forsman H, Fernandez HR, Lindén SK (2015) IL-4 protects the mitochondria against TNFα and IFNγ induced insult during clearance of infection with citrobacter rodentium and Escherichia coli. Scientific Reports 5:15434
Mao P, Reddy PH (2010) Is multiple sclerosis a mitochondrial disease? Biochimica et biophysica acta 1802(1):66–79
Marik C, Felts PA, Bauer J, Lassmann H, Smith KJ (2007) Lesion genesis in a subset of patients with multiple sclerosis: a role for innate immunity? Brain 130(Pt 11):2800–2815
Matsumoto J, Dohgu S, Takata F, Machida T, Bolukbasi Hatip FF, Hatip-Al-Khatib I, Yamauchi A, Kataoka Y (2018) TNF-alpha-sensitive brain pericytes activate microglia by releasing IL-6 through cooperation between IkappaB-NFkappaB and JAK-STAT3 pathways. Brain Res 1692:34–44
Merabova N, Kaminski R, Krynska B, Amini S, Khalili K, Darbinyan A (2012) JCV agnoprotein-induced reduction in CXCL5/LIX secretion by oligodendrocytes is associated with activation of apoptotic signaling in neurons. J Cell Physiol 227(8):3119–3127
Mochida S, Yoshimoto T, Mimura S, Inao M, Matsui A, Ohno A, Koh H, Saitoh E, Nagoshi S, Fujiwara K (2004) Transgenic mice expressing osteopontin in hepatocytes as a model of autoimmune hepatitis. Biochem Biophys Res Commun 317(1):114–120
Moyon S, Dubessy AL, Aigrot MS, Trotter M, Huang JK, Dauphinot L, Potier MC, Kerninon C, Melik Parsadaniantz S, Franklin RJ, Lubetzki C (2015) Demyelination causes adult CNS progenitors to revert to an immature state and express immune cues that support their migration. J Neurosci 35(1):4–20
Okamura RM, Lebkowski J, Au M, Priest CA, Denham J, Majumdar AS (2007) Immunological properties of human embryonic stem cell-derived oligodendrocyte progenitor cells. J Neuroimmunol 192(1-2):134–144
Perry VH, Andersson PB, Gordon S (1993) Macrophages and inflammation in the central nervous system. Trends Neurosci 16(7):268–273
Petkovic F, Campbell IL, Gonzalez B, Castellano B (2017) Reduced cuprizone-induced cerebellar demyelination in mice with astrocyte-targeted production of IL-6 is associated with chronically activated, but less responsive microglia. J Neuroimmunol 310:97–102
Puthalakath H, O'Reilly LA, Gunn P, Lee L, Kelly PN, Huntington ND, Hughes PD, Michalak EM, McKimm-Breschkin J, Motoyama N, Gotoh T, Akira S, Bouillet P, Strasser A (2007) ER stress triggers apoptosis by activating BH3-only protein Bim. Cell 129(7):1337–1349
Ramesh G, Benge S, Pahar B, Philipp MT (2012) A possible role for inflammation in mediating apoptosis of oligodendrocytes as induced by the Lyme disease spirochete Borrelia burgdorferi. J Neuroinflammation 9:72
Richter-Landsberg C, Heinrich M (1996) OLN-93: a new permanent oligodendroglia cell line derived from primary rat brain glial cultures. J Neurosci Res 45(2):161–173
Risker PM, Rifai N, Stampfer MJ, Hennekens CH (2000) Plasma concentration of interleukin-6 and the risk of future myocardial infarction among apparently healthy men. Circulation 101(15):1767–1772
Ruther BJ, Scheld M, Dreymueller D, Clarner T, Kress E, Brandenburg LO, Swartenbroekx T, Hoornaert C, Ponsaerts P, Fallier-Becker P, Beyer C, Rohr SO, Schmitz C, Chrzanowski U, Hochstrasser T, Nyamoya S, Kipp M (2017) Combination of cuprizone and experimental autoimmune encephalomyelitis to study inflammatory brain lesion formation and progression. Glia 65(12):1900–1913
Rutkowski DT, Arnold SM, Miller CN, Wu J, Li J, Gunnison KM, Mori K, Sadighi Akha AA, Raden D, Kaufman RJ (2006) Adaptation to

ER stress is mediated by differential stabilities of pro-survival and pro-apoptotic mRNAs and proteins. PLoS Biol 4(11):e374

Scheld M, Ruther BJ, Grosse-Veldmann R, Ohl K, Tenbrock K, Dreymuller D, Fallier-Becker P, Zendedel A, Beyer C, Clarner T, Kipp M (2016) Neurodegeneration triggers peripheral immune cell recruitment into the forebrain. J Neurosci 36(4):1410–1415

Schlittenhardt D, Schmiedt W, Bonaterra GA, Metz J, Kinscherf R (2005) Colocalization of oxidized low-density lipoprotein, caspase-3, cyclooxygenase-2, and macrophage migration inhibitory factor in arteriosclerotic human carotid arteries. Cell Tissue Res 322(3):425–435

Schonrock LM, Gawlowski G, Bruck W (2000) Interleukin-6 expression in human multiple sclerosis lesions. Neurosci Lett 294(1):45–48

Seino Y, Ikeda U, Ikeda M, Yamamoto K, Misawa Y, Hasegawa T, Kano S, Shimada K (1994) Interleukin 6 gene transcripts are expressed in human atherosclerotic lesions. Cytokine 6(1):87–91

Selvaraju R, Bernasconi L, Losberger C, Graber P, Kadi L, Avellana-Adalid V, Picard-Riera N, Baron Van Evercooren A, Cirillo R, Kosco-Vilbois M, Feger G, Papoian R, Boschert U (2004) Osteopontin is upregulated during in vivo demyelination and remyelination and enhances myelin formation in vitro. Mol Cell Neurosci 25(4):707–721

Škuljec J, Sun H, Pul R, Bénardais K, Ragancokova D, Moharregh-Khiabani D, Kotsiari A, Trebst C, Stangel M (2011) CCL5 induces a pro-inflammatory profile in microglia in vitro. Cellular Immunology 270(2):164–171

Su K, Bourdette D, Forte M (2013) Mitochondrial dysfunction and neurodegeneration in multiple sclerosis. Front Physiol 4:169

Sugiura S, Lahav R, Han J, Kou SY, Banner LR, de Pablo F, Patterson PH (2000) Leukaemia inhibitory factor is required for normal inflammatory responses to injury in the peripheral and central nervous systems in vivo and is chemotactic for macrophages in vitro. Eur J Neurosci 12(2):457–466

Swardfager W, Lanctot K, Rothenburg L, Wong A, Cappell J, Herrmann N (2010) A meta-analysis of cytokines in Alzheimer's disease. Biol Psychiatry 68(10):930–941

Teske N, Liessem A, Fischbach F, Clarner T, Beyer C, Wruck C, Fragoulis A, Tauber SC, Victor M, Kipp M (2018) Chemical hypoxia-induced integrated stress response activation in oligodendrocytes is mediated by the transcription factor nuclear factor (erythroid-derived 2)-like 2 (NRF2). J Neurochem 144(3):285–301

Tezuka T, Tamura M, Kondo MA, Sakaue M, Okada K, Takemoto K, Fukunari A, Miwa K, Ohzeki H, Kano S, Yasumatsu H, Sawa A, Kajii Y (2013) Cuprizone short-term exposure: astrocytic IL-6 activation and behavioral changes relevant to psychosis. Neurobiol Dis 59:63–68

Tsui KH, Chang YL, Feng TH, Chung LC, Lee TY, Chang PL, Juang HH (2012) Growth differentiation factor-15 upregulates interleukin-6 to promote tumorigenesis of prostate carcinoma PC-3 cells. J Mol Endocrinol 49(2):153–163

Tzartos JS, Friese MA, Craner MJ, Palace J, Newcombe J, Esiri MM, Fugger L (2008) Interleukin-17 production in central nervous system-infiltrating T cells and glial cells is associated with active disease in multiple sclerosis. Am J Pathol 172(1):146–155

van der Valk P, Amor S (2009) Preactive lesions in multiple sclerosis. Curr Opin Neurol 22(3):207–213

Wang CH, Wu SB, Wu YT, Wei YH (2013) Oxidative stress response elicited by mitochondrial dysfunction: implication in the pathophysiology of aging. Exp Biol Med (Maywood) 238(5):450–460

Wruck CJ, Streetz K, Pavic G, Gotz ME, Tohidnezhad M, Brandenburg LO, Varoga D, Eickelberg O, Herdegen T, Trautwein C, Cha K, Kan YW, Pufe T (2011) Nrf2 induces interleukin-6 (IL-6) expression via an antioxidant response element within the IL-6 promoter. J Biol Chem 286(6):4493–4499

Wuerfel J, Bellmann-Strobl J, Brunecker P, Aktas O, McFarland H, Villringer A, Zipp F (2004) Changes in cerebral perfusion precede plaque formation in multiple sclerosis: a longitudinal perfusion MRI study. Brain 127(Pt 1):111–119

Yang P, Wen H, Ou S, Cui J, Fan D (2012) IL-6 promotes regeneration and functional recovery after cortical spinal tract injury by reactivating intrinsic growth program of neurons and enhancing synapse formation. Exp Neurol 236(1):19–27

Yang R, Lirussi D, Thornton TM, Jelley-Gibbs DM, Diehl SA, Case LK, Madesh M, Taatjes DJ, Teuscher C, Haynes L, Rincon M (2015) Mitochondrial Ca(2)(+) and membrane potential, an alternative pathway for Interleukin 6 to regulate CD4 cell effector function. Elife 4

Yumoto K, Ishijima M, Rittling SR, Tsuji K, Tsuchiya Y, Kon S, Nifuji A, Uede T, Denhardt DT, Noda M (2002) Osteopontin deficiency protects joints against destruction in anti-type II collagen antibody-induced arthritis in mice. Proc Natl Acad Sci U S A 99(7):4556–4561

Zeis T, Probst A, Steck AJ, Stadelmann C, Bruck W, Schaeren-Wiemers N (2009) Molecular changes in white matter adjacent to an active demyelinating lesion in early multiple sclerosis. Brain Pathol 19(3):459–466

Zhang X, Tachibana S, Wang H, Hisada M, Williams GM, Gao B, Sun Z (2010) Interleukin-6 is an important mediator for mitochondrial DNA repair after alcoholic liver injury in mice. Hepatology 52(6):2137–2147

9. Literaturverzeichnis

Balabanov, R., Strand, K., Goswami, R., McMahon, E., Begolka, W., Miller, S. D. and Popko, B. (2007) Interferon-gamma-oligodendrocyte interactions in the regulation of experimental autoimmune encephalomyelitis. J Neurosci 27, 2013-2024.

Barnett, M. H. and Prineas, J. W. (2004) Relapsing and remitting multiple sclerosis: pathology of the newly forming lesion. Ann Neurol 55, 458-468.

Bradl, M. and Lassmann, H. (2010) Oligodendrocytes: biology and pathology. Acta Neuropathol 119, 37-53.

Bramow, S., Frischer, J. M., Lassmann, H., Koch-Henriksen, N., Lucchinetti, C. F., Sorensen, P. S. and Laursen, H. (2010) Demyelination versus remyelination in progressive multiple sclerosis. Brain 133, 2983-2998.

Bruce, C. C., Zhao, C. and Franklin, R. J. (2010) Remyelination - An effective means of neuroprotection. Horm Behav 57, 56-62.

Cannella, B. and Raine, C. S. (2004) Multiple sclerosis: cytokine receptors on oligodendrocytes predict innate regulation. Ann Neurol 55, 46-57.

Cao, S. S. and Kaufman, R. J. (2014) Endoplasmic reticulum stress and oxidative stress in cell fate decision and human disease. Antioxid Redox Signal 21, 396-413.

Clarner, T., Diederichs, F., Berger, K., Denecke, B., Gan, L., van der Valk, P., Beyer, C., Amor, S. and Kipp, M. (2012) Myelin debris regulates inflammatory responses in an experimental demyelination animal model and multiple sclerosis lesions. Glia 60, 1468-1480.

Cui, Q. L., Kuhlmann, T., Miron, V. E., Leong, S. Y., Fang, J., Gris, P., Kennedy, T. E., Almazan, G. and Antel, J. (2013) Oligodendrocyte progenitor cell susceptibility to injury in multiple sclerosis. Am J Pathol 183, 516-525.

De Groot, C. J., Bergers, E., Kamphorst, W., Ravid, R., Polman, C. H., Barkhof, F. and van der Valk, P. (2001) Post-mortem MRI-guided sampling of multiple sclerosis brain lesions: increased yield of active demyelinating and (p)reactive lesions. Brain 124, 1635-1645.

di Penta, A., Moreno, B., Reix, S. et al. (2013) Oxidative stress and proinflammatory cytokines contribute to demyelination and axonal damage in a cerebellar culture model of neuroinflammation. PLoS One 8, e54722.

Draheim, T., Liessem, A., Scheld, M. et al. (2016) Activation of the astrocytic Nrf2/ARE system ameliorates the formation of demyelinating lesions in a multiple sclerosis animal model. Glia 64, 2219-2230.

Edagawa, M., Kawauchi, J., Hirata, M., Goshima, H., Inoue, M., Okamoto, T., Murakami, A., Maehara, Y. and Kitajima, S. (2014) Role of activating transcription factor 3 (ATF3) in endoplasmic reticulum (ER) stress-induced sensitization of p53-deficient human colon cancer cells to tumor necrosis factor (TNF)-related apoptosis-inducing ligand (TRAIL)-mediated apoptosis through up-regulation of death receptor 5 (DR5) by zerumbone and celecoxib. J Biol Chem 289, 21544-21561.

Gay, F. W., Drye, T. J., Dick, G. W. and Esiri, M. M. (1997) The application of multifactorial cluster analysis in the staging of plaques in early multiple sclerosis. Identification and characterization of the primary demyelinating lesion. Brain 120 (Pt 8), 1461-1483.

Gehrmann, J., Matsumoto, Y. and Kreutzberg, G. W. (1995) Microglia: intrinsic immuneffector cell of the brain. Brain Res Brain Res Rev 20, 269-287.

Haider, L., Fischer, M. T., Frischer, J. M. et al. (2011) Oxidative damage in multiple sclerosis lesions. Brain 134, 1914-1924.

Itoh, K., Wakabayashi, N., Katoh, Y., Ishii, T., O'Connor, T. and Yamamoto, M. (2003) Keap1 regulates both cytoplasmic-nuclear shuttling and degradation of Nrf2 in response to electrophiles. Genes Cells 8, 379-391.

Kipp, M., Nyamoya, S., Hochstrasser, T. and Amor, S. (2017) Multiple sclerosis animal models: a clinical and histopathological perspective. Brain Pathol 27, 123-137.

Kozutsumi, Y., Segal, M., Normington, K., Gething, M. J. and Sambrook, J. (1988) The presence of malfolded proteins in the endoplasmic reticulum signals the induction of glucose-regulated proteins. Nature 332, 462-464.

Li, G. L., Farooque, M., Holtz, A. and Olsson, Y. (1999) Apoptosis of oligodendrocytes occurs for long distances away from the primary injury after compression trauma to rat spinal cord. Acta Neuropathol 98, 473-480.
Lin, M. T. and Beal, M. F. (2006) Mitochondrial dysfunction and oxidative stress in neurodegenerative diseases. Nature 443, 787-795.
Liu, B., Chen, X., Wang, Z. Q. and Tong, W. M. (2014) DNA damage and oxidative injury are associated with hypomyelination in the corpus callosum of newborn Nbn(CNS-del) mice. J Neurosci Res 92, 254-266.
Liu, B. and Li, Z. (2008) Endoplasmic reticulum HSP90b1 (gp96, grp94) optimizes B-cell function via chaperoning integrin and TLR but not immunoglobulin. Blood 112, 1223-1230.
Marciniak, S. J., Yun, C. Y., Oyadomari, S., Novoa, I., Zhang, Y., Jungreis, R., Nagata, K., Harding, H. P. and Ron, D. (2004) CHOP induces death by promoting protein synthesis and oxidation in the stressed endoplasmic reticulum. Genes Dev 18, 3066-3077.
Moyon, S., Dubessy, A. L., Aigrot, M. S. et al. (2015) Demyelination causes adult CNS progenitors to revert to an immature state and express immune cues that support their migration. J Neurosci 35, 4-20.
Ohl, K., Tenbrock, K. and Kipp, M. (2016) Oxidative stress in multiple sclerosis: Central and peripheral mode of action. Exp Neurol 277, 58-67.
Okamura, R. M., Lebkowski, J., Au, M., Priest, C. A., Denham, J. and Majumdar, A. S. (2007) Immunological properties of human embryonic stem cell-derived oligodendrocyte progenitor cells. J Neuroimmunol 192, 134-144.
Pakos-Zebrucka, K., Koryga, I., Mnich, K., Ljujic, M., Samali, A. and Gorman, A. M. (2016) The integrated stress response. EMBO Rep 17, 1374-1395.
Pantoni, L., Garcia, J. H. and Gutierrez, J. A. (1996) Cerebral white matter is highly vulnerable to ischemia. Stroke 27, 1641-1646; discussion 1647.
Patrikios, P., Stadelmann, C., Kutzelnigg, A. et al. (2006) Remyelination is extensive in a subset of multiple sclerosis patients. Brain 129, 3165-3172.
Perry, V. H., Andersson, P. B. and Gordon, S. (1993) Macrophages and inflammation in the central nervous system. Trends Neurosci 16, 268-273.
Plemel, J. R., Liu, W. Q. and Yong, V. W. (2017) Remyelination therapies: a new direction and challenge in multiple sclerosis. Nat Rev Drug Discov 16, 617-634.
Prineas, J. W. and Parratt, J. D. (2012) Oligodendrocytes and the early multiple sclerosis lesion. Ann Neurol 72, 18-31.
Puthalakath, H., O'Reilly, L. A., Gunn, P. et al. (2007) ER stress triggers apoptosis by activating BH3-only protein Bim. Cell 129, 1337-1349.
Ramesh, G., Benge, S., Pahar, B. and Philipp, M. T. (2012) A possible role for inflammation in mediating apoptosis of oligodendrocytes as induced by the Lyme disease spirochete Borrelia burgdorferi. J Neuroinflammation 9, 72.
Reth, M. (2002) Hydrogen peroxide as second messenger in lymphocyte activation. Nat Immunol 3, 1129-1134.
Rosenzweig, S. and Carmichael, S. T. (2013) Age-dependent exacerbation of white matter stroke outcomes: a role for oxidative damage and inflammatory mediators. Stroke 44, 2579-2586.
Rutkowski, D. T., Arnold, S. M., Miller, C. N. et al. (2006) Adaptation to ER stress is mediated by differential stabilities of pro-survival and pro-apoptotic mRNAs and proteins. PLoS Biol 4, e374.
Santos, C. X., Tanaka, L. Y., Wosniak, J. and Laurindo, F. R. (2009) Mechanisms and implications of reactive oxygen species generation during the unfolded protein response: roles of endoplasmic reticulum oxidoreductases, mitochondrial electron transport, and NADPH oxidase. Antioxid Redox Signal 11, 2409-2427.
Scheld, M., Fragoulis, A., Nyamoya, S. et al. (2018) Mitochondrial Impairment in Oligodendroglial Cells Induces Cytokine Expression and Signaling. J Mol Neurosci.
Sim, F. J., Zhao, C., Penderis, J. and Franklin, R. J. (2002) The age-related decrease in CNS remyelination efficiency is attributable to an impairment of both oligodendrocyte progenitor recruitment and differentiation. J Neurosci 22, 2451-2459.
Slowik, A., Schmidt, T., Beyer, C., Amor, S., Clarner, T. and Kipp, M. (2015) The sphingosine 1-phosphate receptor agonist FTY720 is neuroprotective after cuprizone-induced CNS demyelination. Br J Pharmacol 172, 80-92.

Smith, H. L. and Mallucci, G. R. (2016) The unfolded protein response: mechanisms and therapy of neurodegeneration. Brain 139, 2113-2121.
Tzartos, J. S., Friese, M. A., Craner, M. J., Palace, J., Newcombe, J., Esiri, M. M. and Fugger, L. (2008) Interleukin-17 production in central nervous system-infiltrating T cells and glial cells is associated with active disease in multiple sclerosis. Am J Pathol 172, 146-155.
Uranova, N., Orlovskaya, D., Vikhreva, O., Zimina, I., Kolomeets, N., Vostrikov, V. and Rachmanova, V. (2001) Electron microscopy of oligodendroglia in severe mental illness. Brain Res Bull 55, 597-610.
van der Valk, P. and Amor, S. (2009) Preactive lesions in multiple sclerosis. Curr Opin Neurol 22, 207-213.
van der Vlies, D., Makkinje, M., Jansens, A., Braakman, I., Verkleij, A. J., Wirtz, K. W. and Post, J. A. (2003) Oxidation of ER resident proteins upon oxidative stress: effects of altering cellular redox/antioxidant status and implications for protein maturation. Antioxid Redox Signal 5, 381-387.
Vostrikov, V., Orlovskaya, D. and Uranova, N. (2008) Deficit of pericapillary oligodendrocytes in the prefrontal cortex in schizophrenia. World J Biol Psychiatry 9, 34-42.
Wakabayashi, N., Itoh, K., Wakabayashi, J. et al. (2003) Keap1-null mutation leads to postnatal lethality due to constitutive Nrf2 activation. Nat Genet 35, 238-245.
Witte, M. E., Mahad, D. J., Lassmann, H. and van Horssen, J. (2014) Mitochondrial dysfunction contributes to neurodegeneration in multiple sclerosis. Trends Mol Med 20, 179-187.
Wuerfel, J., Bellmann-Strobl, J., Brunecker, P., Aktas, O., McFarland, H., Villringer, A. and Zipp, F. (2004) Changes in cerebral perfusion precede plaque formation in multiple sclerosis: a longitudinal perfusion MRI study. Brain 127, 111-119.
Zeis, T., Probst, A., Steck, A. J., Stadelmann, C., Bruck, W. and Schaeren-Wiemers, N. (2009) Molecular changes in white matter adjacent to an active demyelinating lesion in early multiple sclerosis. Brain Pathol 19, 459-466.

10. Danksagung

In Liebe für Johanna und für meine Familie, ohne deren Unterstützung und Rückhalt weder mein Studium noch diese Arbeit möglich gewesen wären.

Mein Dank gilt meinem Doktorvater Prof. Dr. med. Dr. rer. nat. Markus Kipp für die hervorragenden Forschungsbedingungen, kontinuierliche Unterstützung und Geduld sowie Hilfe in meiner wissenschaftlichen Ausbildung. Vielen Dank für die hervorragende Betreuung und Zusammenarbeit.

Weiterhin möchte ich allen weiteren Mitgliedern der Anatomischen Anstalt Lehrstuhl II - Neuroanatomie danken, insbesondere Sarah Wübbel, die mich mit großer Geduld in die Zellkultur eingeführt hat und immer für Fragen zur Verfügung stand. Außerdem möchte ich mich für die gute Zusammenarbeit bei allen Doktoranden bedanken, die auf alle meine wissenschaftlichen Fragen eingegangen sind und jederzeit Teamgeist bewiesen haben. Ich möchte Beate Aschauer und Astrid Baltruschat für ihre produktive und freundschaftliche Zusammenarbeit danken. Für die Möglichkeit, an der Anatomischen Anstalt promovieren zu dürfen, danke ich Prof. Dr. med. Christoph Schmitz.